

## REPORT 1313

# EXPLORATORY INVESTIGATION OF BOUNDARY-LAYER TRANSITION ON A HOLLOW CYLINDER AT A MACH NUMBER OF 6.9<sup>†</sup>

By MITCHEL H. BERTRAM

### SUMMARY

*The Reynolds number for transition on the outside of a hollow cylinder with heat transfer from the boundary layer to the wall has been investigated at a Mach number of 6.9 in the Langley 11-inch hypersonic tunnel. The type of boundary layer was determined from impact-pressure surveys and optical viewing. From a correlation of results obtained from various sources at lower Mach numbers (in the range 2.0 to 4.5) and data from the present tests with variable Reynolds number per inch, leading-edge thickness and free-stream Reynolds number per inch appear to be important considerations in flat-plate transition results. At a given Mach number, it appears that the Reynolds number based on leading-edge thickness is an important parameter that must be considered in comparisons of flat-plate transition data from various installations.*

### INTRODUCTION

The importance of obtaining extensive regions of laminar flow on surfaces in very high-speed flight does not have to be emphasized. Certain theoretical analyses indicate a decrease in the critical Reynolds number for transition with Mach number (Lees and Lin in refs. 1 and 2 and Van Driest's calculations, ref. 3, based on the Lees-Lin theory). A recent paper by Dunn and Lin (ref. 4) removes some of the limitations of the Lees-Lin theory mainly by the inclusion of three-dimensional disturbances and the demonstration that the stability characteristics can depend on temperature fluctuations. According to this theory, at Mach numbers between 1 and 2 three-dimensional disturbances begin to play the leading role in many problems of practical interest, and at supersonic Mach numbers the boundary layer can never be completely stabilized with respect to all three-dimensional disturbances. For Mach numbers up to about 2, however, cooling of the solid surface is found to be effective in stabilizing the boundary layer. Although calculations were not made, this general conclusion would apparently remain unchanged for Mach numbers up to perhaps 6; however, for Mach numbers above about 2 Dunn and Lin do not believe their present method of numerical calculations to be adequate.

The theoretical prediction that an increase in Mach number should decrease the stability (from the Lees-Lin theory)

was substantiated to the extent that the earlier experimental work on bodies at the lower supersonic Mach numbers (as in a 1951 paper by Potter, ref. 5) showed a decrease in transition Reynolds number with increasing Mach number. An extrapolation of these early data indicated Reynolds numbers for transition that were quite low compared with the Reynolds numbers obtained with bodies and wings tested in the Langley 11-inch hypersonic tunnel at Mach number 6.9 (for example, refs. 6 and 7). However, the models tested in the 11-inch hypersonic tunnel have an appreciable heat transfer from the boundary layer to the model surface and, in addition, the Reynolds number per unit length is considerably higher than would be obtained by an extrapolation of Potter's data.

On the basis of experimentally determined trends, Potter in reference 8 revised his earlier observations to include the estimated effects of factors such as wall temperature and tunnel-air density. Though admittedly crude in application, Potter's modifications to wind-tunnel cone-cylinder results to allow for wall-temperature and density effects resulted in reasonable agreement with free-flight data from bodies of revolution as compiled by Gazley in reference 9. More recent contributions have been the original work and compilations by Czarnecki and Sinclair (refs. 10 and 11) who have investigated the effects of Mach number, body shape, heat transfer, surface roughness, and angle of attack. Although the work of the various investigators has resulted in some progress, there still does not exist a coherent picture of the various factors affecting transition nor a definite idea of what the Reynolds number for transition will be at various Mach numbers and other varying conditions.

The present exploratory investigation was initiated in 1951 to provide preliminary information on boundary-layer transition in the hypersonic range. A hollow cylinder was chosen for the test configuration because of advantages in mounting and lack of tip effects. Because the Langley 11-inch hypersonic tunnel has only a short running time, the wall temperature of the cylinder, which was initially at about room temperature, was not controlled. The wall temperature obtained was thus a result of the heat transfer during the run from the boundary layer on both the inside and the outside of the cylinder. An attempt was also made to correlate the

<sup>†</sup> Supersedes NACA Technical Note 3546 by Mitchel H. Bertram, 1956.

available transition data on cylinders and flat plates by use of nondimensional parameters involving the pressure and the leading-edge thickness.

**SYMBOLS**

$M$	Mach number
$m$	exponent in power law for velocity
$p_t'$	total pressure measured by pitot tube
$p_t$	supply pressure
$p_\infty$	free-stream pressure
$N_{Pr}$	Prandtl number
$r$	radial distance from tunnel axis (see sketch 1)
$R_x$	Reynolds number based on distance from leading edge
$R_{x_T}$	Reynolds number based on distance from leading edge to transition location
$R_t$	Reynolds number based on leading-edge thickness
$t$	leading-edge thickness
$T$	absolute temperature
$u$	velocity
$x$	distance measured from cylinder leading edge, axially along cylinder surface
$y$	distance normal to cylinder surface, measured from surface
$X$ $Y$ $Z$ } $X_{LE}$	nozzle coordinates (see sketch 1)
$\delta$	boundary-layer thickness
$\eta = \frac{y}{x} \sqrt{R_x}$	
$\phi$	angle about $X$ axis of nozzle in $Z$ - $Y$ plane (see sketch 1)
$\rho$	density
$\mu$	dynamic viscosity
$\tau$	time
Subscripts:	
*	ratio of local conditions to conditions in undisturbed free stream
$\infty$	refers to conditions in undisturbed free stream
$w$	refers to conditions at wall

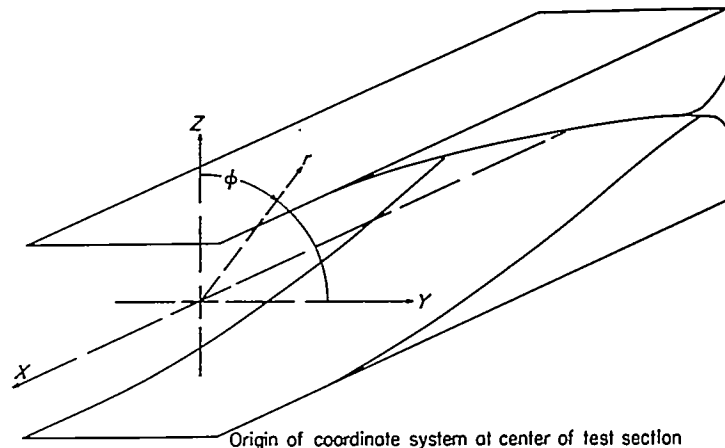
**APPARATUS AND METHODS**

**TUNNEL AND NOZZLES**

This investigation was conducted in the Langley 11-inch hypersonic tunnel, an intermittent tunnel with running time of 70 seconds for these tests. These tests utilized two two-dimensional nozzles both of which provide a Mach number of slightly less than 7. The first nozzle had contours machined from steel and was replaced after the tests had started by a nozzle having contours constructed of Invar. Invar was used for the contour plates of the second nozzle in order to

alleviate the deflection of the first minimum which occurred in the steel nozzle because of differential heating of the nozzle blocks. In addition, the nozzle was designed so that pressure gradients normal to the horizontal plane of symmetry were a minimum.

The variation of free-stream Mach number with longitudinal distance in the steel and in the Invar nozzle is shown in figures 1 and 2 for time 60 seconds after the start of the test run. The center of the test section is taken as the origin of the coordinate system, as shown in sketch 1. In



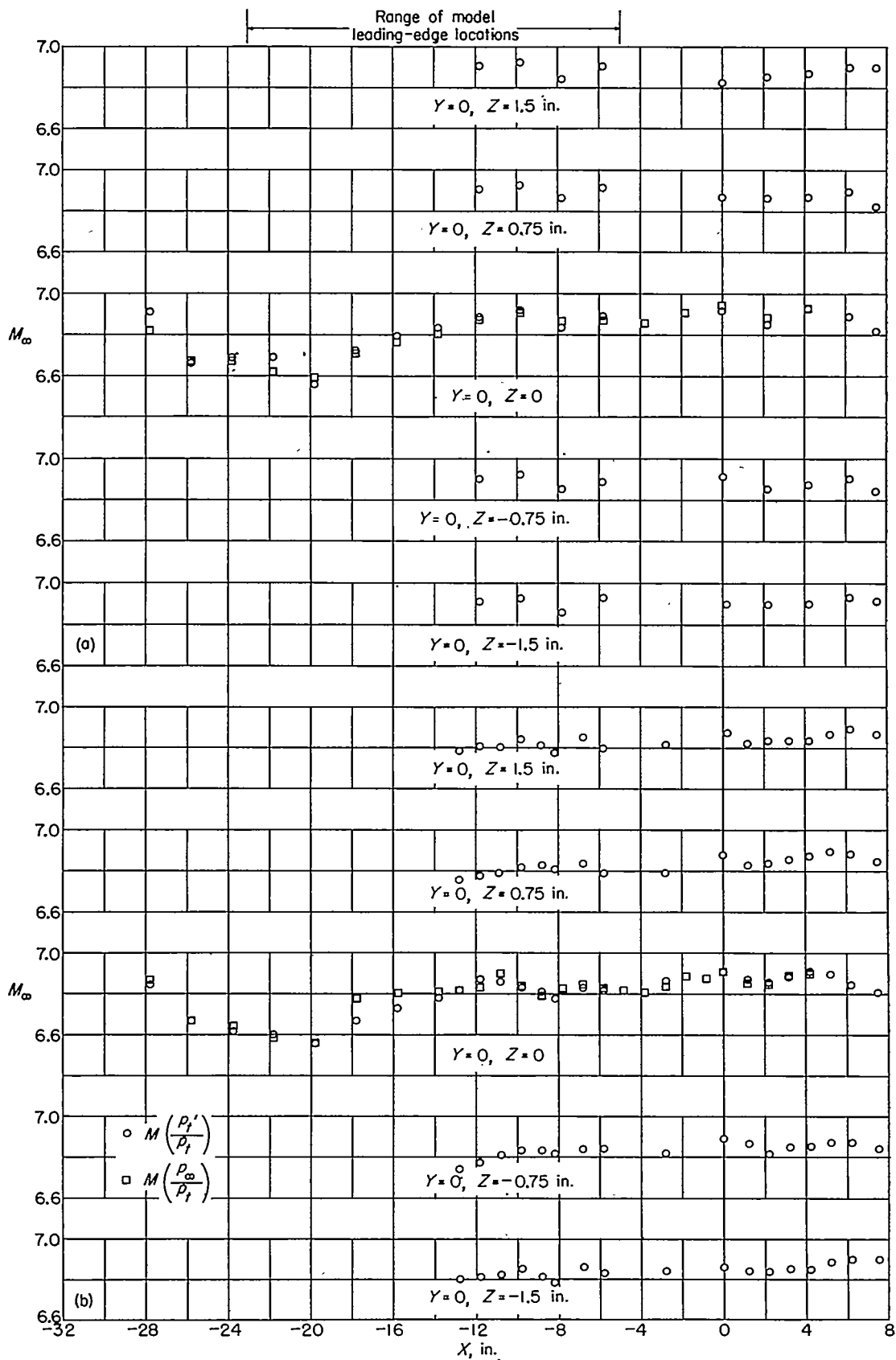
Sketch 1.

contrast to the steel nozzle in which the test-section Mach number changed about 2.5 percent in the period of time from 10 to 70 seconds after the start of the run, the Mach number in the Invar nozzle changed only 1 percent during this same period of time. A description of the tunnel may be found in reference 12 and a description of the steel nozzle and a more complete calibration at a stagnation pressure of 25 atmospheres in reference 13.

Boundary-layer-survey tests were conducted at supply pressures of 25 and 33 atmospheres (Reynolds number per inch of about  $0.26 \times 10^6$  and  $0.34 \times 10^6$ , respectively<sup>1</sup>). Optical viewing was used to obtain data with supply pressures in the range from 14 to 37 atmospheres. Pressure-fluctuation measurements were taken in the settling chamber with a flush diaphragm gage which had a flat response to fluctuations with a frequency from 4 to 2000 cps. The recorded fluctuations of air pressure were approximately the same whether the gage was open to the tunnel air or blanked off so that the tunnel air could not directly affect the gage face (about  $\pm 0.1$  inch mercury at frequencies from 1000 to 2000 cps). Thus, either the frequency of the actual pressure fluctuations was considerably greater than those to which the gage would respond accurately or the magnitude of the fluctuations was less than the electrical noise level of the instrumentation setup.

<sup>1</sup> The viscosity used to obtain the Reynolds numbers is based on the Sutherland formula:

$$\mu_\infty = 0.0220 \frac{T_\infty^{3/2}}{T_\infty + 177^\circ\text{F}} \times 10^5 \frac{\text{lb-sec}}{\text{sq ft}}$$



(a)  $p_t = 33.4$  atmospheres.

(b)  $p_t = 25$  atmospheres.

FIGURE 1.—Longitudinal Mach number distribution in steel nozzle at two pressure levels (60 seconds after start of test run).

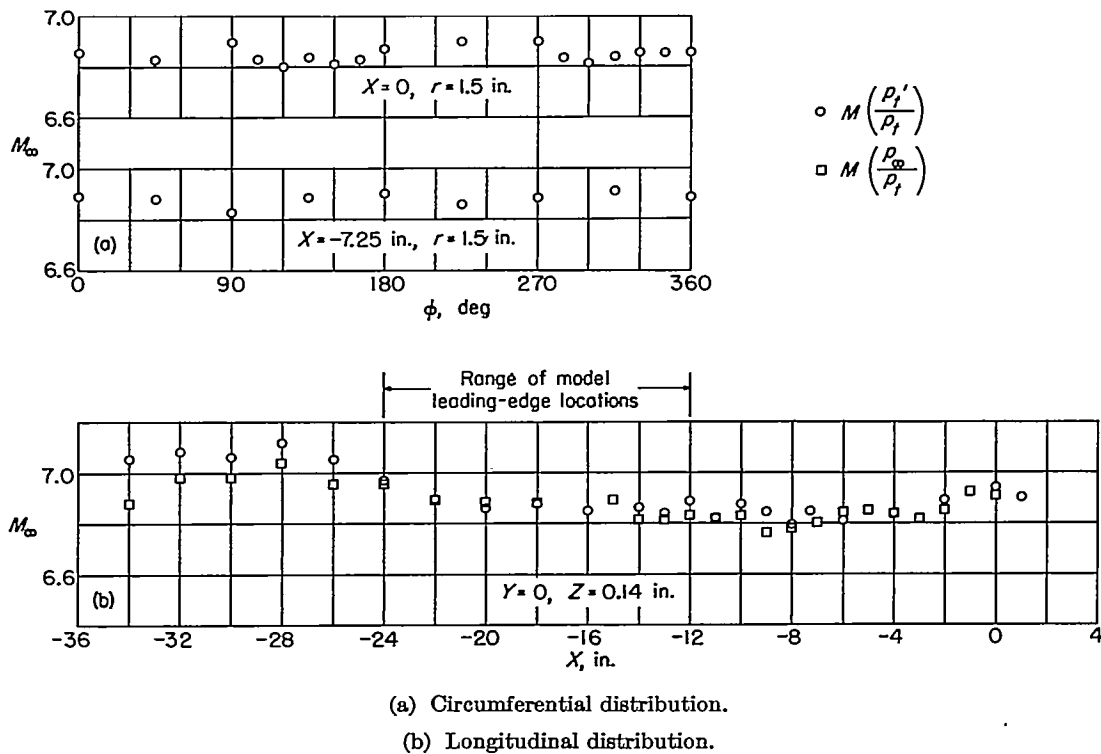


FIGURE 2.—Mach number distribution in Invar nozzle at a supply pressure of 30 atmospheres (80 seconds after start of test run).

During most of these tests, the tunnel was operated at a stagnation temperature of about  $1,135^\circ$  R, although stagnation temperatures for some runs were as high as  $1,180^\circ$  R and for a few others were as low as  $1,100^\circ$  R. In the earliest tests, the air was heated by means of the storage heater described in references 12 and 13. This heater was replaced in later tests by an electrical heater with Nichrome tube resistance elements. Measurements of the temperature fluctuations in the settling chamber and in the test section when the resistance heater was used were made with a chromel-alumel thermocouple formed of No. 40 wire (0.0031-inch diam.) in series with an adjacent thermocouple of No. 18 wire (0.040-inch diam.) with reversed polarity. The observed temperature fluctuations can be described approximately as a wave with a frequency of 2 to 4 cps and an amplitude of  $5^\circ$  to  $15^\circ$  upon which is superimposed another wave with a frequency of 10 to 15 cps and an amplitude of  $1^\circ$  F to  $2^\circ$  F. The settling-chamber and test-section measurements were in agreement as to magnitude and approximate frequency of occurrence of the fluctuations. There was no apparent difference between temperature fluctuation results obtained at 25 and 33 atmospheres.

#### MODELS AND PROBES

**Models.**—The models were hollow cylinders for which the diameter and method of mounting are shown in figure 3. The cylinders were made from seamless steel tubing machined

and polished longitudinally on the outside and cleaned on the inside, with the leading edge beveled on the inside. The leading-edge thickness was determined by viewing the leading edge through a calibrated microscope.

Surface roughness was measured with a profilometer. Movement of the stylus in the longitudinal direction along the outside surface of the cylinder indicated a surface roughness with root-mean-square values generally of 3 microinches with occasional values of 6 microinches. Lateral traverse of the surface at right angles to the direction of the polishing indicated a root-mean-square surface roughness of about 10 microinches. Such surface-roughness measurements as these are highly questionable, however, in view of the experience of Jedlicka, Wilkins, and Seiff (ref. 14, page 6) when using such a stylus type of instrument. Photographs of the surface at a magnification of  $20\times$  indicated that most scratches on the surface ran in the longitudinal direction. The width of the scratches seen on these photographs were between 0.0002 and 0.0005 inch and numbered about 800 to the inch of width.

One hollow cylinder had a portion of the outer surface knurled near the leading edge. As a general description the knurling was in a diamond pattern with the lateral dimension of the diamond about  $\frac{1}{2}$  inch and the longitudinal dimension about  $\frac{3}{4}$  inch. This knurling started approximately  $\frac{1}{2}$  inch from the leading edge, covered about 2 inches

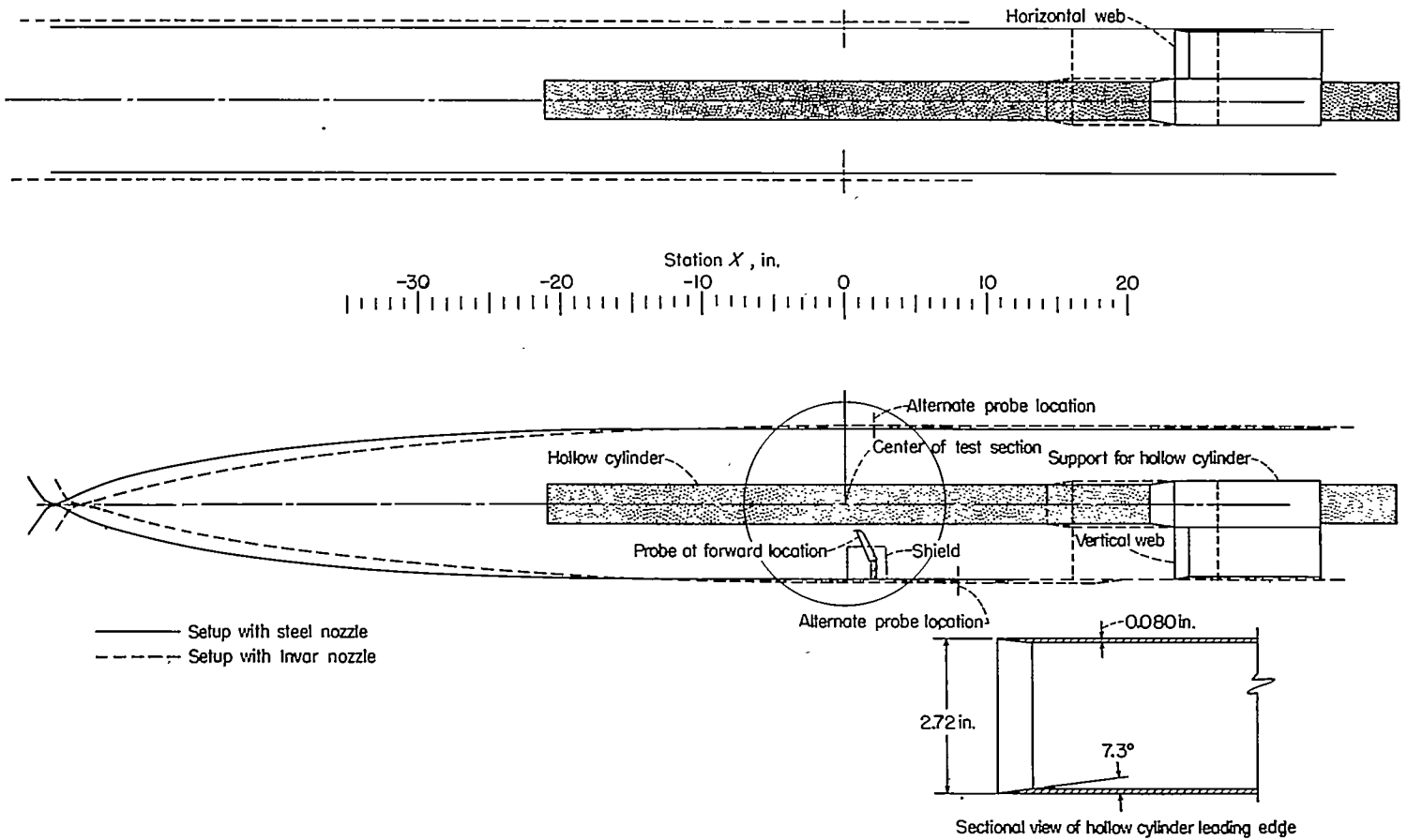


FIGURE 3.—Mounting and location of hollow cylinder and probe in steel and Invar nozzles.

of cylinder length including a tapered portion of about  $\frac{1}{4}$  inch at each end, extended above the original surface about 0.005 inch, and was indented about 0.003 inch. In the unknurled half inch of length at the leading edge the outer surface was actually at an angle of about  $0.8^\circ$  exposed to the free-stream flow; otherwise the cylinder was as described previously.

Another cylinder was tested with glass tape wrapped about a portion of the outer surface. This tape was 0.007 inch thick and started 4 inches behind the hollow cylinder leading edge and extended for 1.25 inches.

**Probes.**—A pressure probe with a flattened tip typical of the type used in the present tests is shown in figure 4. A number of these probes were made for replacement purposes, as they occasionally broke in use. The first of these probes to be made had an outside dimension of the minor axis of about 0.015 inch. With more experience in making them, it became practical to construct probes with minor-axis outside dimensions of 0.006 to 0.010 inch. A further reduction in this dimension was deemed undesirable because of anticipated difficulties with pressure lag when the probe was located close to the surface of the cylinder in a laminar

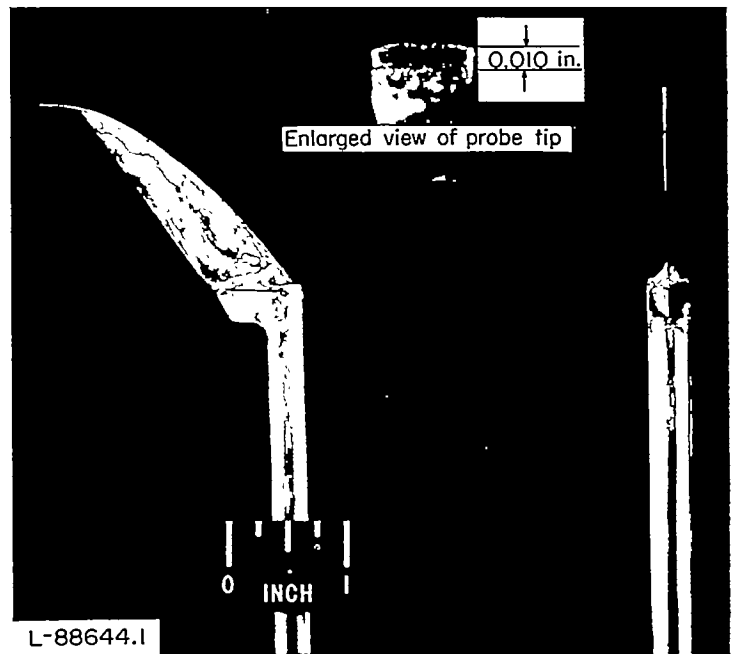


FIGURE 4.—Typical impact-pressure probe with flattened tip.

boundary layer. Some early tests were conducted with the probe formed from unflattened 0.040-outside-diameter by 0.020-inside-diameter tubing. The supporting web for this probe was unswept and considerably broader than the web shown in figure 4.

For the tests in the steel nozzle, the probes were mounted on a 3/8-inch-diameter steel tube (shown in fig. 4); whereas, for the tests in the Invar nozzle, the tube was 1/4 inch in diameter. The probe could be located in several positions in the test section as shown in figure 3.

The pressures in the impact tube were measured by means of the aneroid recording units described in reference 12. Most of the pressures were measured with an error of about 1 percent, although the error in some cases was 2 or 3 percent.

Heating effects on models and probes, and accuracy of setting vertical distance.—The reference setting of the probe ( $y=0$ ) was made visually by sighting through the test section at an illuminated diffusing screen, masked to a suitable size. The probe was moved toward the cylinder until the light passing between the probe tip and the cylinder was observed without magnifying aids to disappear, and the probe was then backed off from the cylinder until the light could be barely observed. At the stagnation temperature of these runs (about 675° F) there was a relative deflection of the probe and the cylinder during the running time. The first run in each series at a given station was used to calibrate this relative deflection by having the operator of the traverse mechanism keep the probe substantially fixed with relation to the cylinder and recording the deflection indicated by the scale of the traversing head as a function of time. In order to keep this deflection due to heating to a minimum, the steel tube on which the probe was mounted was shielded from the airstream as shown in figure 3. Corrections to the initial setting were made according to the observed deflection. The accuracy with which the operator could follow the relative deflection of the probe and model is believed, in general, to be within 0.002 inch, judging from a comparison of repeat runs of the deflection calibration.

**OPTICAL VIEWING**

Optical viewing by both shadowgraph and schlieren methods was used to examine the flow over the cylinders. The schlieren system had a vertical Z-shape light path with a horizontal knife edge. Schlieren photographs were obtained by using either continuous lighting with a shutter speed of 1/150 second or flash exposures of 2 to 3 microseconds duration. In order to obtain shadowgraphs photographic paper was simply placed in the parallel beam of the schlieren system. This technique necessitated exposures of about 2 seconds duration because of the low light density.

**MODEL TEMPERATURE**

At the start of a run, the model has an isothermal surface with a ratio of wall temperature to stream temperature of about 5.0. With sufficient running time to attain equilibrium,

a ratio of wall temperature to stream temperature of about 9.0 would be expected for stations away from the leading edge with a laminar boundary layer and about 9.4 with a turbulent boundary layer.

The initial rates of change of model temperature with time  $dT_w/d\tau$  determined from theory for laminar and turbulent boundary layers and for boundary layers with transition occurring at various Reynolds numbers is shown in figure 5. Also shown is the assumed rate of change of  $T_w$  with time used to calculate the wall temperature for the determination of various parameters in the boundary layer from the impact pressure measurements. The value of  $dT_w/d\tau$  was assumed constant throughout the running time with no consideration given to longitudinal heat conduction. A few experimental measurements of which the accuracy left much to be desired indicated the assumed curve to be reasonable; although the assumed  $dT_w/d\tau$  is expected on the average to be too high at the more forward stations and too low at the most rearward stations. The maximum error in the assumed wall temperature is expected to be about 15 percent and this deviation should not have a significant effect on the computations for the reduction of the total-pressure ratio to velocity ratio for present purposes.

**RESULTS AND DISCUSSION**

Presented in figure 6 are the impact-pressure profiles obtained in both the steel and the Invar nozzles 60 seconds after the start of the tests at a Reynolds number per inch of about  $0.34 \times 10^6$  (supply pressure of 33 atmospheres). In this figure each data point represents the pressure at 60 seconds from the start of one test run. These data are summarized in table I. The theoretical curves shown in figure 6 are those for a laminar boundary layer on a flat plate calculated

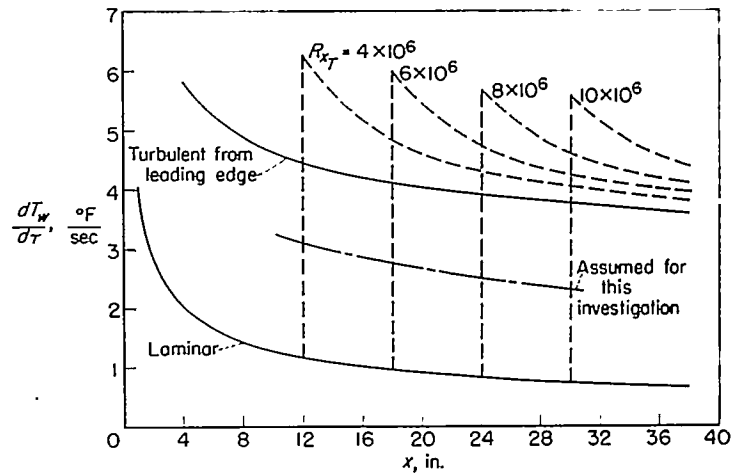


FIGURE 5.—Initial rate of change of wall temperature with time as a function of distance from the nose of a flat plate. Plate material steel, 0.040 inch thick, heated through one surface, insulated on opposite surface.  $\frac{T_w}{T_\infty} = 5$ ;  $M_\infty = 6.9$ ;  $\frac{R_x}{x} = 0.33 \times 10^6$  per inch.

TABLE I.—SUMMARY OF RESULTS FROM STEEL AND INVAR NOZZLES

$$\left[ M=6.9; \frac{R_x}{x}=0.34 \times 10^6 \text{ per inch} \right]$$

Figure	$R_x$	$X_{LB}$ , in.	Surface condition	Type of boundary layer
(a) Steel Nozzle				
6(a)	$4.1 \times 10^6$	-10.8	Tape	Laminar
		-11.2	Smooth	Laminar
		-11.2	Smooth	Laminar
		-11.1	Knurled	Laminar
		-11.0	Knurled	Laminar
		-11.2	Knurled	Turbulent
6(b)	$6.2 \times 10^6$	-11.2	Knurled	Turbulent
		-11.2	Smooth	Transitional
		-17.2	Tape	Incipient transition
		-17.2	Smooth	Incipient transition
6(c)	$7.1 \times 10^6$	-17.1	Knurled	Laminar <sup>1</sup>
		-17.1	Knurled	Transitional <sup>1</sup>
		-14.2	Smooth	Transitional <sup>1</sup>
		-14.7	Smooth	Turbulent <sup>1</sup>
6(d)	$8.1 \times 10^6$	-17.2	Smooth	Turbulent
		-17.9	Smooth	Turbulent
		-23.1	Knurled	Incipient transition <sup>1</sup>
		-23.0	Knurled	Turbulent <sup>1</sup>
6(e)	$9.0 \times 10^6$	-20.2	Knurled	Turbulent
		-20.9	Smooth	Turbulent
6(f)	$10.1 \times 10^6$	-23.2	Knurled	Turbulent
(b) Invar Nozzle				
6(a)	$4.1 \times 10^6$	-12.0	Smooth	Turbulent <sup>1</sup>
		-12.0	Smooth	Laminar <sup>1</sup>
		-12.0	Smooth	Turbulent
6(b)	$6.2 \times 10^6$	-18.0	Smooth	Transitional <sup>1</sup>
		-18.0	Smooth	Turbulent <sup>1</sup>
6(d)	$8.1 \times 10^6$	-18.0	Smooth	Turbulent
		-24.0	Smooth	Turbulent

<sup>1</sup> Anomalous cases.

by the Crocco method as presented by Van Driest (ref. 15). The effect of Prandtl number, wall temperature, and velocity profile shape on these curves is discussed in more detail in Appendix A to this report.

If for the moment certain anomalies which appear in the data and differences in cylinder surface condition are ignored, certain overall results are evident. With the leading edge of the cylinder located at about the -11-inch station in the steel nozzle (figs. 6 (a) and (b)), transition is found to occur between a Reynolds number of  $4 \times 10^6$  and  $6 \times 10^6$ . A value of  $R_x=4.1 \times 10^6$  corresponds to a Reynolds number based on momentum thickness of about 1,720 from the measured pressures. With the leading edge at approximately the -17-inch station in the steel nozzle (figs. 6 (b) and (d)),

transition appears to occur in general between a Reynolds number of about  $6 \times 10^6$  and  $8 \times 10^6$ . One set of data from the steel nozzle at a Reynolds number of about  $8 \times 10^6$  (fig. 6 (d)) with the leading edge set at the -23-inch station appears to indicate incipient transition. Less data were obtained in the Invar nozzle (figs. 6 (a), (b), and (d)) than in the steel nozzle, but the data apparently do not show the large variations in profile shape with cylinder location found in the steel nozzle. In this nozzle transition apparently occurred before a Reynolds number of  $4 \times 10^6$  (fig. 6 (a)), at least for one set of test data.

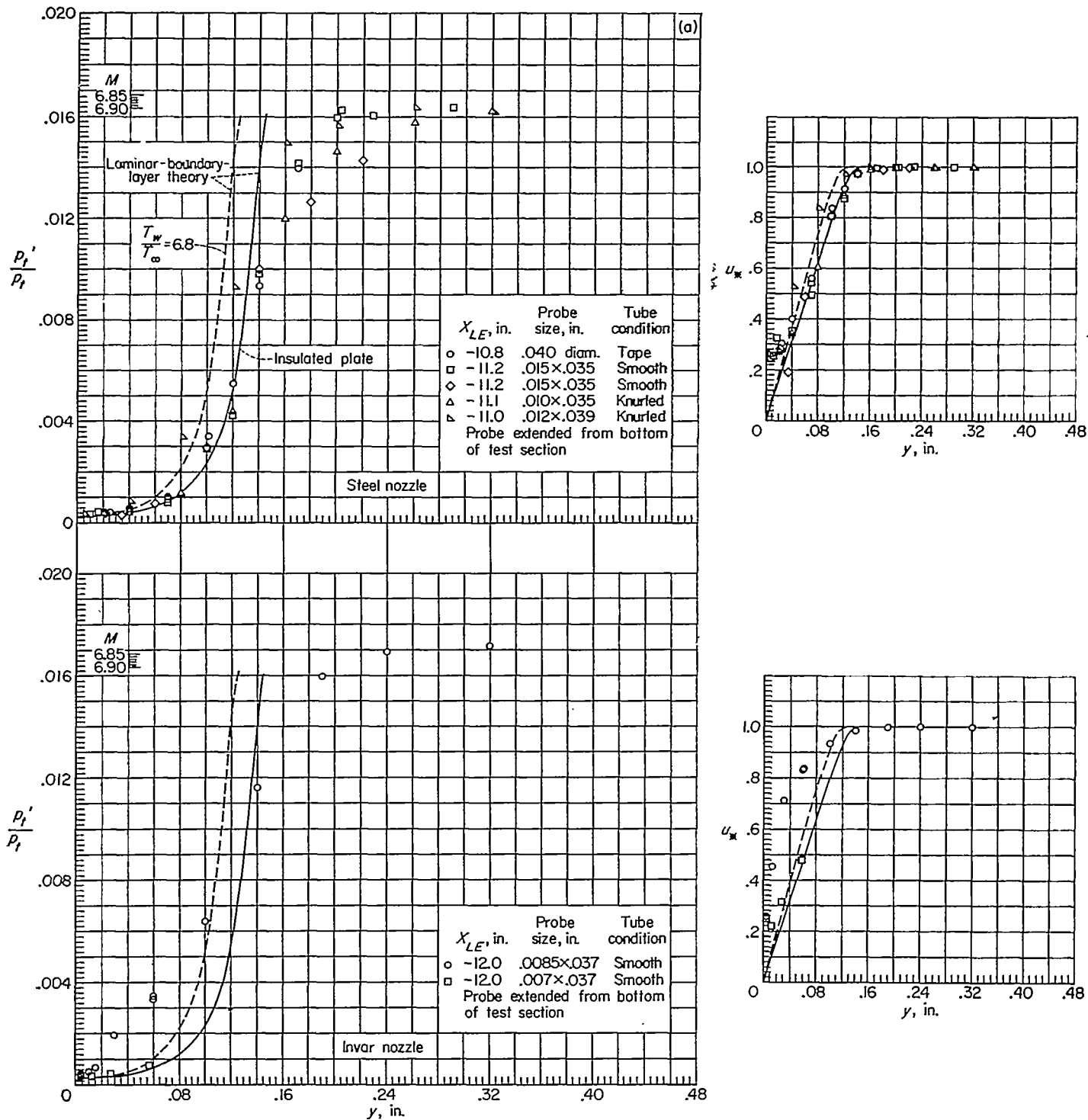
Possible explanations for this behavior are discussed in the following sections together with a discussion of the previously dismissed anomalies and other factors.

#### FACTORS INFLUENCING TRANSITION

**Effect of model location.**—The preceding discussion has implied an effect of model location on the Reynolds numbers for transition obtained in the steel nozzle. The cylinder leading-edge locations shown in figure 6 and table I can be associated with the Mach number (pressure) gradients indicated by figures 1 and 2. Take the cylinder locations shown in figure 6 (b), for example; in the steel nozzle with  $X_{LB} \approx -17$  inches, the forward part of the cylinder was in a region with a considerable length of negative  $dp/dX$  on the nozzle center line; whereas with the cylinder farther downstream in the nozzle ( $X_{LB} \approx -11$  inches) there is a short length of positive  $dp/dX$  on the nozzle center line in the leading-edge region. As previously noted, in general, the farther upstream the location of the leading edge in the steel nozzle the higher the transition Reynolds number appeared to be. In the Invar nozzle at these same stations the pressure gradient on the nozzle center line is considerably smaller. The results from the Invar nozzle do not indicate a noteworthy effect of model location on transition.

Although other factors enter into the problem the improved Mach number (pressure) distribution in the Invar nozzle is probably an important reason for the decreased Reynolds number for transition observed in this nozzle. In the Invar nozzle the model apparently did not protrude into a region of relatively strong negative pressure gradient as was the case in the steel nozzle for the model positions for which the pressure profiles indicated the highest Reynolds number for transition.

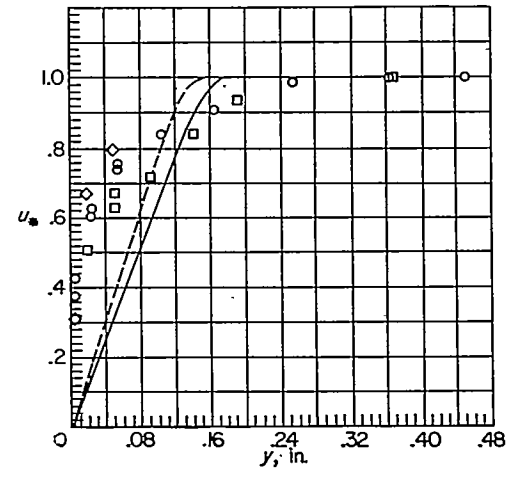
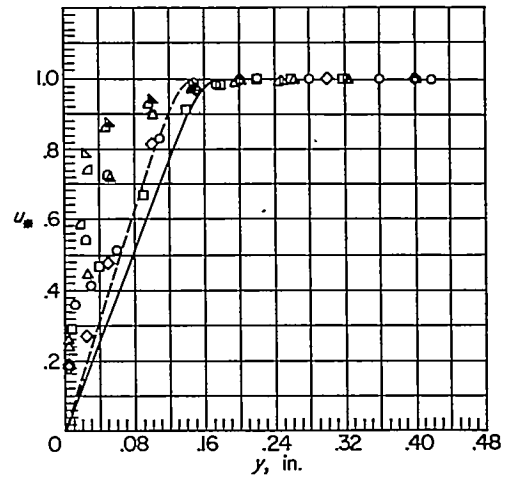
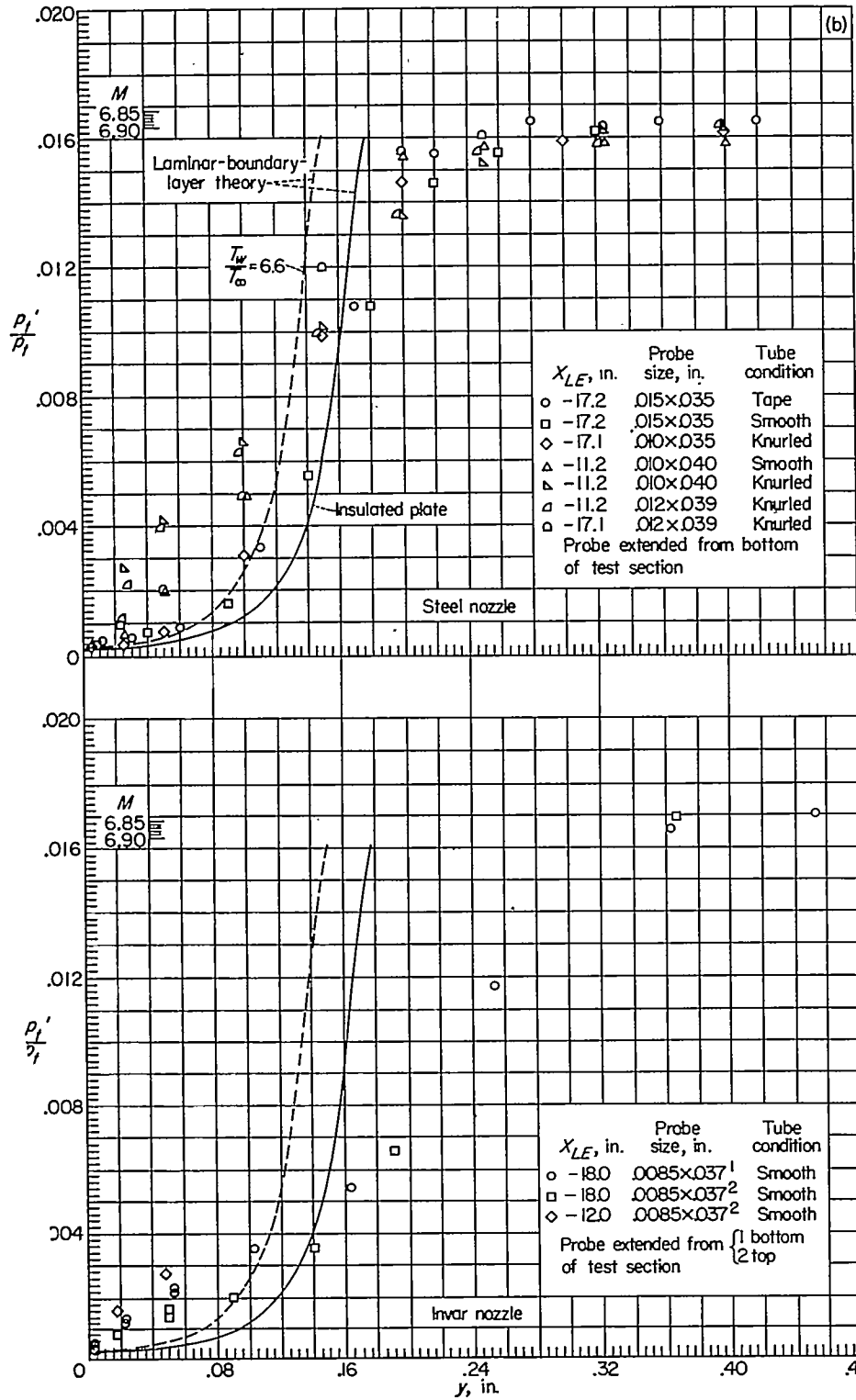
Another consideration in the effect of model location is flow angularity in the nozzle; however, at present little can be said concerning this effect. A calibration of the steel nozzle indicates that flow angles in the test section where the model surface is located may be as much as  $0.5^\circ$ , and the flow angles average to about  $0.2^\circ$  in this region (ref. 13, fig. 13). With the model located at a given station in the nozzle the effects of flow angularity would be considered to be fixed; however, in a comparison of the results at various model locations, some flow-angularity effects could exist.



(a)  $x = 12$  in. ( $R_x = 4.1 \times 10^6$ ).

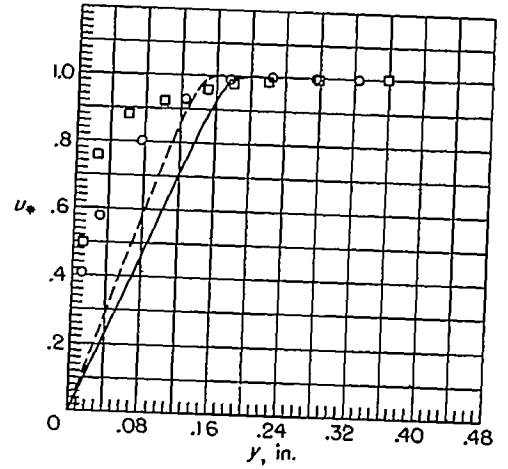
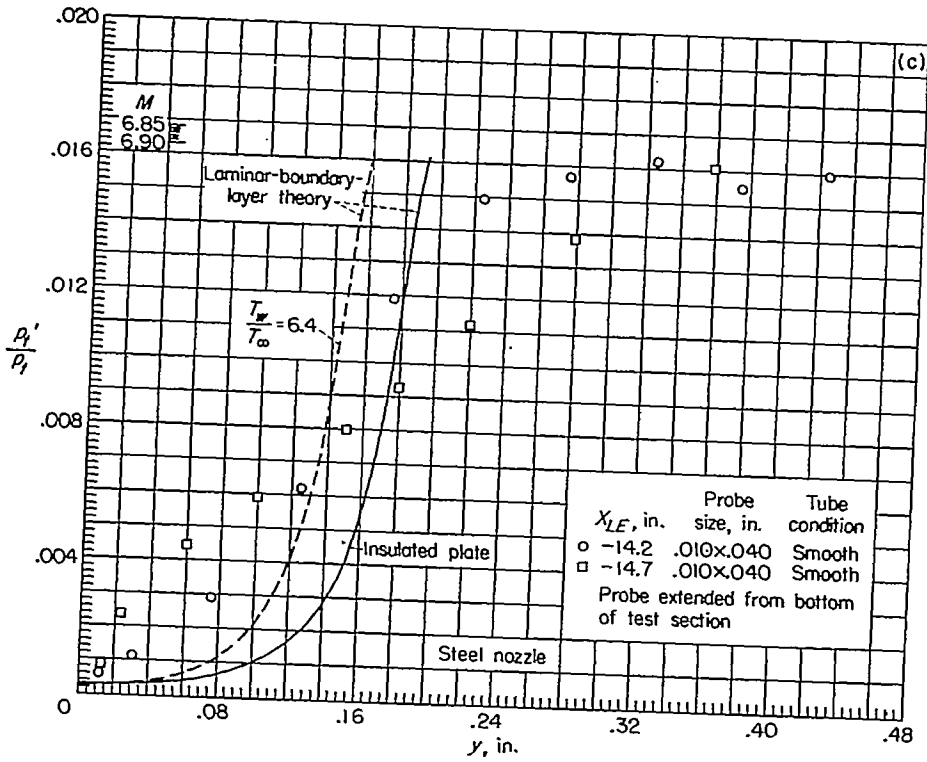
FIGURE 6.—Impact pressure and velocity distributions in boundary layer.





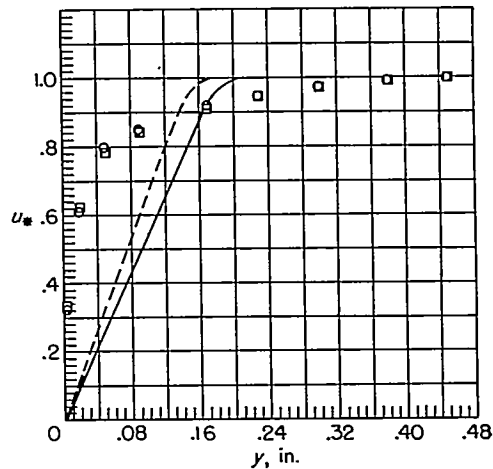
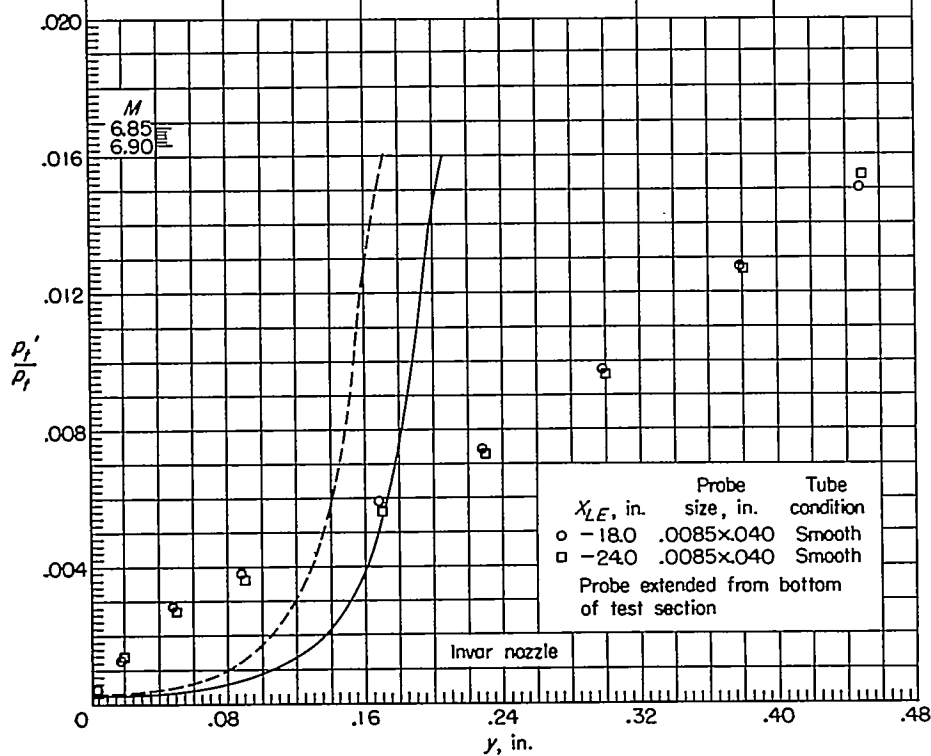
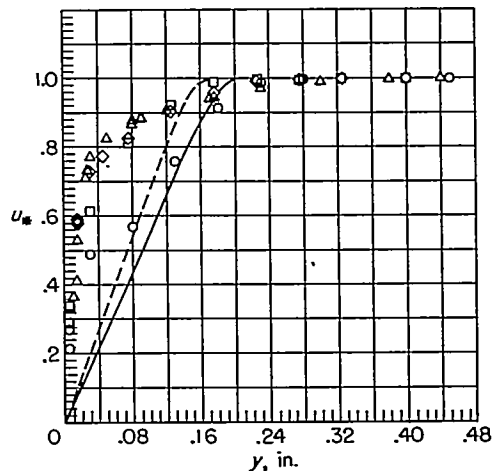
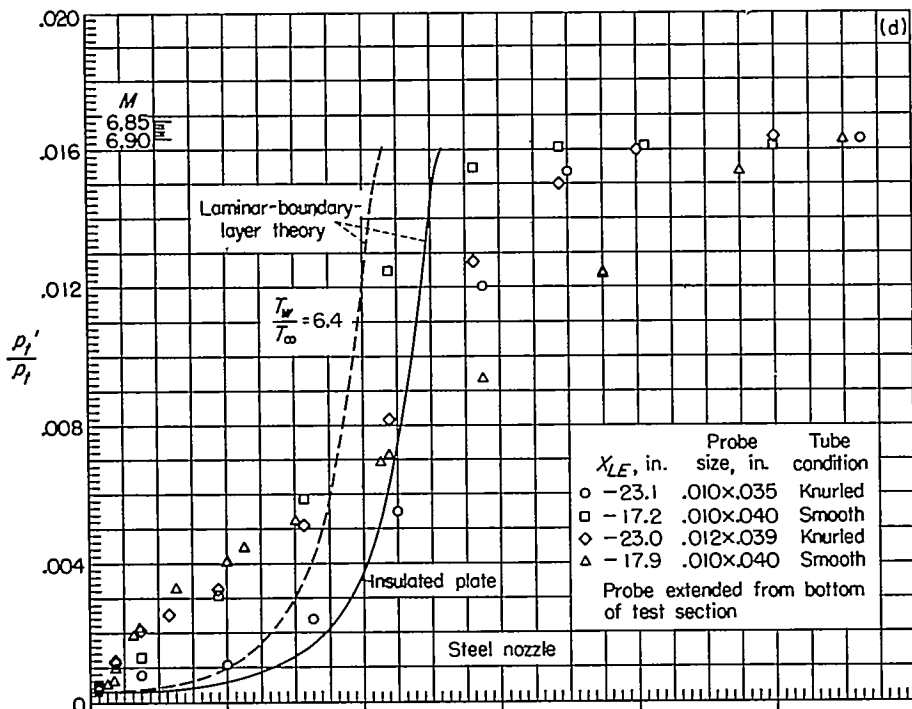
(b)  $x=18$  in. ( $R_x=6.2 \times 10^6$ ).

FIGURE 6.—Continued.



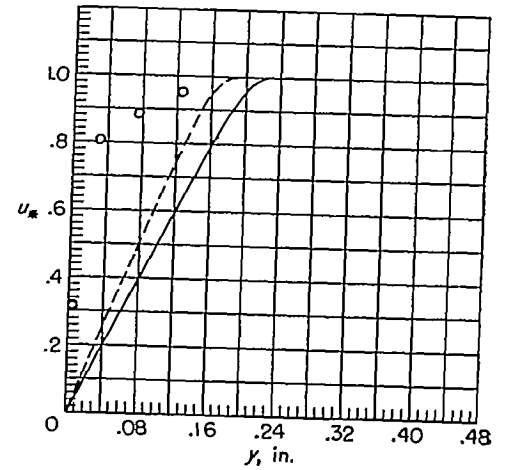
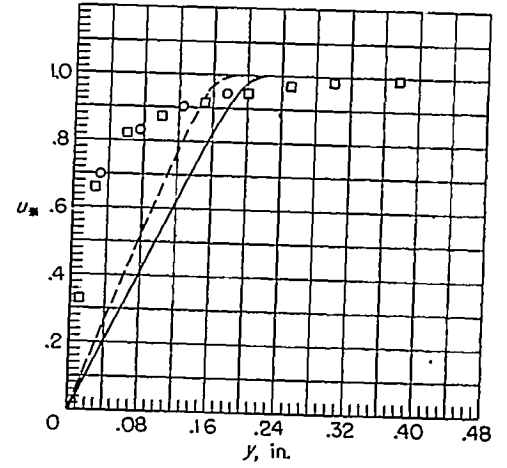
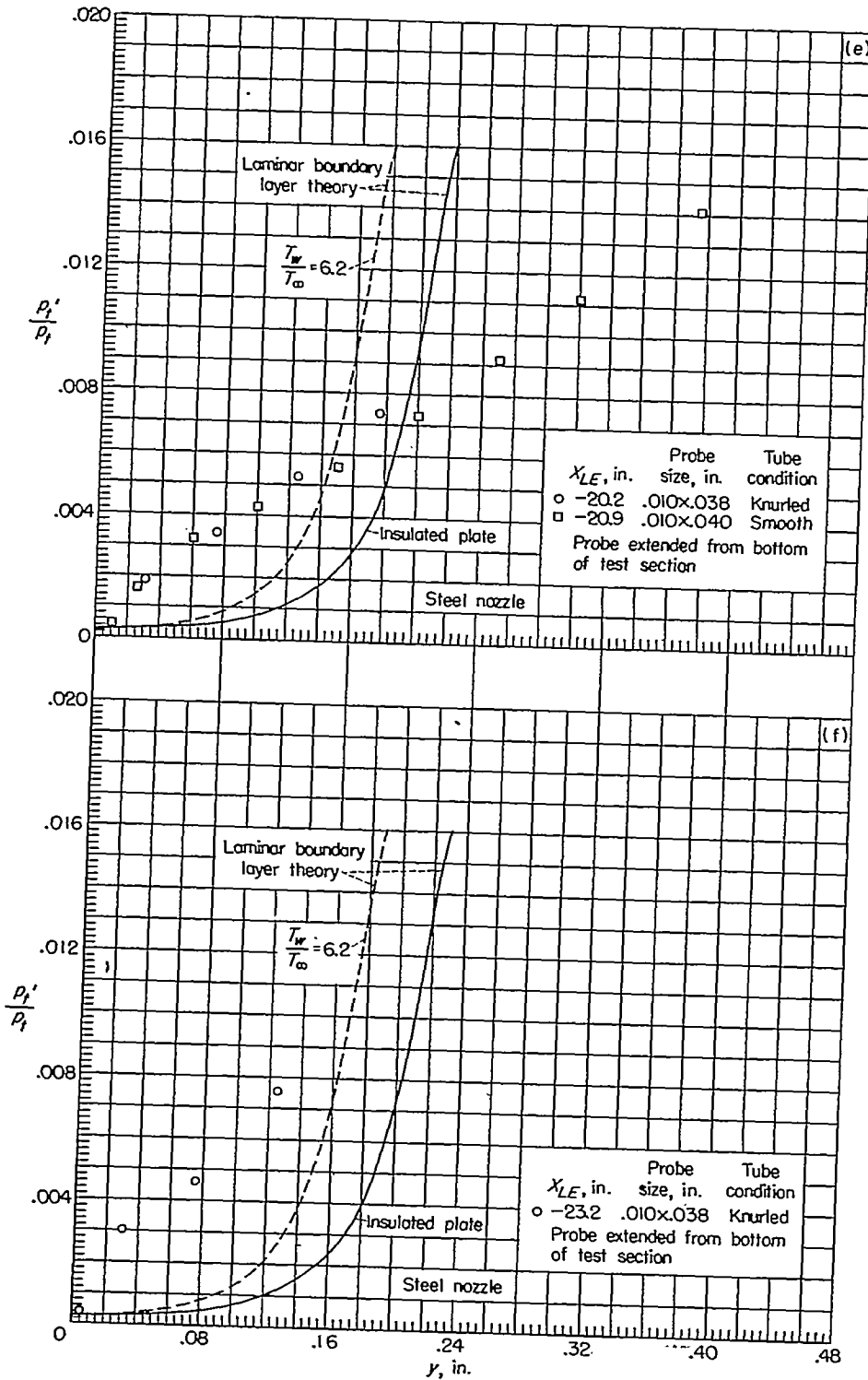
(c)  $x = 21$  in. ( $R_x = 7.1 \times 10^6$ ).

FIGURE 6.—Continued.



(d)  $x = 2\frac{1}{2}$  in. ( $R_x = 8.1 \times 10^6$ ).

FIGURE 6.—Continued.



(e)  $x=27$  in. ( $R_x=9.0 \times 10^6$ ).

(f)  $x=30$  in. ( $R_x=10.1 \times 10^6$ ).

FIGURE 6.—Concluded.

Effects of model angle of attack would also be expected to be fixed. However, the misalignment of the cylinder with respect to the tunnel axis was less than about 3 minutes and the effect of such a misalignment would be expected to be negligible.

**Effect of surface condition.**—The correlation of tests at the lower supersonic Mach numbers has indicated two important parameters in the effect of surface roughness on boundary-layer transition (refs. 10 and 14). These are the ratio of roughness height to a characteristic boundary-layer thickness and the ratio of molecular mean-free-path length to roughness height; however, much concerning these effects is still speculation. Consider first the taped cylinder described under the section entitled "Models". The ratio of tape thickness to boundary-layer displacement thickness was about 0.08. The ratio of tape thickness to mean free path is about 230 in the stream, 35 at the wall, and 18 as a minimum a little distance from the wall. Conditions at and near the wall are expected to be the best criteria for molecular mean-free-path considerations. From consideration of both boundary-layer thickness and molecular mean free path, the tape would not be expected to have an effect and this appears to be substantiated in figures 6 (a) and 6 (b).

The other variation in surface condition on the cylinders tested was knurling near the leading edge. According to the lower speed correlations of roughness height to boundary layer height (ratio 0.18 at start of knurling based on crest to mean surface height), the knurling could have an effect on transition of the boundary layer (ref. 10, figs. 6 and 7); however, from mean-free-path considerations it is doubtful that such an effect would occur. Actually the data indicating what is probably the highest Reynolds number for transition (see fig. 6(d)) were obtained on the cylinder with knurling. However, the data from the knurled cylinder are not consistent in this regard (see fig. 6 (b)). There is the possibility that the high Reynolds number for transition indicated in figure 6 (d) is associated in part with the slight bevel inadvertently formed on the surface at the leading edge. (See the description of the models in a previous section.) Lee (ref. 16) found that a 10° external bevel on a hollow cylinder, tested at Mach numbers of 2.15 and 3.25, increased the Reynolds number for transition by 50 to 60 percent over that obtained when the outer surface was unbroken to the leading edge; however, the external bevel in the present model is only about 0.8°.

**Effect of leading-edge thickness.**—A possible cause for certain anomalies in the transition Reynolds number obtained from measurement of the boundary-layer pitot-pressure profile (as shown in table I) is the variation of leading-edge thickness circumferentially around the leading edge. In this case the leading-edge thickness varied between 0.001 and 0.003 inch around the leading edge. The following discussion forms a possible explanation for these anomalies.

Two of the more obvious effects inherent in a finite leading-edge thickness which can possibly affect the Reynolds

number for transition are as follows: First, temperature increases across the strong leading-edge shock and results in an initially low value of Reynolds number per inch; second, the pressure is initially high but there is a negative gradient in pressure and in surface Reynolds number per unit length, with the pressure becoming essentially equal to stream static pressure at a sufficient distance from the leading edge. The boundary layer is thin near the leading edge and can therefore be affected considerably by the disturbance due to the finite thickness of the leading edge. It appears that the Reynolds number based on leading-edge thickness  $R_t$  is the correct parameter to describe the effect of the leading edge on the boundary layer. A plausible argument is that for low Reynolds numbers per unit length or small leading-edge thicknesses, or both (low  $R_t$ ), the boundary layer quickly becomes thick enough so that the effect of the leading-edge thickness is small; that is, the boundary layer quickly grows out of the region where the main influence is from the strong shock at the leading edge; whereas for larger leading-edge thicknesses or high Reynolds numbers per unit length, or both (high  $R_t$ ), the boundary layer is thinner and is affected by the leading edge for a considerably greater distance in terms, say, of boundary-layer thicknesses. Thus, with Reynolds number based on undisturbed free-stream Reynolds number per inch, the Reynolds number for transition  $R_{x_T}$  might be expected to increase with  $R_t$ .

As the Mach number increases a third factor may become increasingly significant. This factor is the effect of the boundary layer itself in producing a shock and inducing a pressure gradient augmenting the effects due to leading-edge thickness. The effect of leading-edge thickness and boundary-layer thickness at  $M=6.9$  on the pressures on a flat plate has been reported in reference 18, and these results show that rather large increases in surface pressure with a considerable negative pressure gradient can be ascribed to a combination of leading-edge thickness and boundary-layer-displacement effects.

The previously available data from various sources (refs. 18 to 23) for the variation in transition Reynolds number with the dimensional parameters, Reynolds number per inch and leading-edge thickness, are shown in figure 7 (a). The trend of the data from the various installations is obviously similar whether the parameter varied is Reynolds number per unit length or leading-edge thickness. An increase in either Reynolds number per inch or leading-edge thickness gives an increase in the Reynolds number for transition. In this respect the data obtained in the present experiments in the steel nozzle (fig. 7 (b)) are similar in trend to the results at lower Mach numbers shown in figure 7 (a). The only set of data obtained without movement of the model between tests is shown by the circular symbols in figure 7 (b) where the leading-edge thickness was in the range from 0.003 to 0.005 inch. These shadowgraph data indicate a Reynolds number from transition varying from about  $1.3 \times 10^6$  at a Reynolds number per inch of  $0.14 \times 10^6$

to about  $3.7 \times 10^6$  at a Reynolds number per inch of  $0.40 \times 10^6$ , so that the distance from the leading edge at which transition occurs is indicated to be relatively unaffected by changes in Reynolds number per inch (as obtained mainly by varying the stagnation pressure). Other shadowgraphs from test runs with the cylinder leading edge located 18 inches upstream of the center of the test section corroborated the plotted shadowgraph data to the extent that the start of transition was indicated to be outside the area of view afforded by the test section windows that is some distance less than 12 inches from the cylinder leading edge. The appearance of the phenomena which were interpreted to provide the data shown in figure 7 (b) is shown in figure 8. Figure 8 (a) is included to show the forward part of the model and the appearance of a known laminar boundary layer. Figures 8 (b) to 8 (d) show flow phenomena that are interpreted as boundary-layer transition by various methods of viewing, whereas figures 8 (e) and 8 (f) show the cylinder with the leading edge far forward in the nozzle. At the lower Reynolds number (fig. 8 (e)) the flow is apparently laminar for an appreciable distance in the field of view. This phenomenon is the anomalous result shown by the triangular symbol in figure 7 (b) where a Reynolds number for transition of about  $5.7 \times 10^6$  is indicated at a Reynolds number per inch of  $0.25 \times 10^6$ . At the higher Reynolds number (fig. 8 (f)) the appearance of the boundary layer is changed and the thickness is considerably increased. This change is interpreted to represent transitional and turbulent boundary layer over the entire field of view. The photograph shown as figure 8 (f) was obtained during the set of tests for which data are designated by the circular symbol for the steel nozzle in figure 6 (d). When several photographs were obtained by the flash schlieren method during a given run, all indicated essentially the same Reynolds number for transition. Figure 8 (g) is a flash schlieren photograph obtained immediately after the shadowgraph runs with the model unchanged from the  $X_{LE} = -18.0$ -inch position mentioned previously. From the diffuse appearance of the boundary layer, transition is indicated to have occurred ahead of the portion of the cylinder in the viewing area; thus, there is at least qualitative agreement, in this case also, between results obtained by these two methods of viewing.

The data shown in figure 7 (a) are presented in figure 9 with the Reynolds number for transition  $R_{x_T}$  in this case plotted as a function of the nondimensional parameter, Reynolds number based on leading-edge thickness  $R_l$ . Some secondary effects are indicated by the data of Brinich and Diaconis (ref. 23); however, in general, this set of data correlates reasonably well. As can be seen, the increase in transition Reynolds numbers can be quite large. This same trend is shown by results presented in figure 7 of reference 24, but sufficient quantitative data are not available to include these test results in figure 9.

Clearly, in an endeavor to correlate the available data, certain factors which could prevent correlation have been neglected; among these is the turbulence level of the tunnel air. The data of Brinich and Diaconis (ref. 23) are useful in this connection in a comparison with recent data obtained by Brinich (ref. 25). The main difference in the conditions under which the two sets of data were obtained is in a modification to the air-supply chamber of the Lewis 1- by 1-foot variable Reynolds number wind tunnel to improve the turbulence level of the flow entering the nozzle. These data are shown in figure 10. The increase in the Reynolds number for transition from the latest data (ref. 25) is quite evident. Within the individual sets of data a trend of increasing Reynolds number for transition with increasing Reynolds number per inch can be detected. This is the same trend that Ross (ref. 26) observed on a cone tested in the same wind tunnel. A more detailed study of transition on a cone in this tunnel (ref. 27) has indicated not only an overall change in turbulence level between the two sets of data associated with the tunnel modification but in addition secondary changes in turbulence level resulting from variations in Reynolds number per inch.

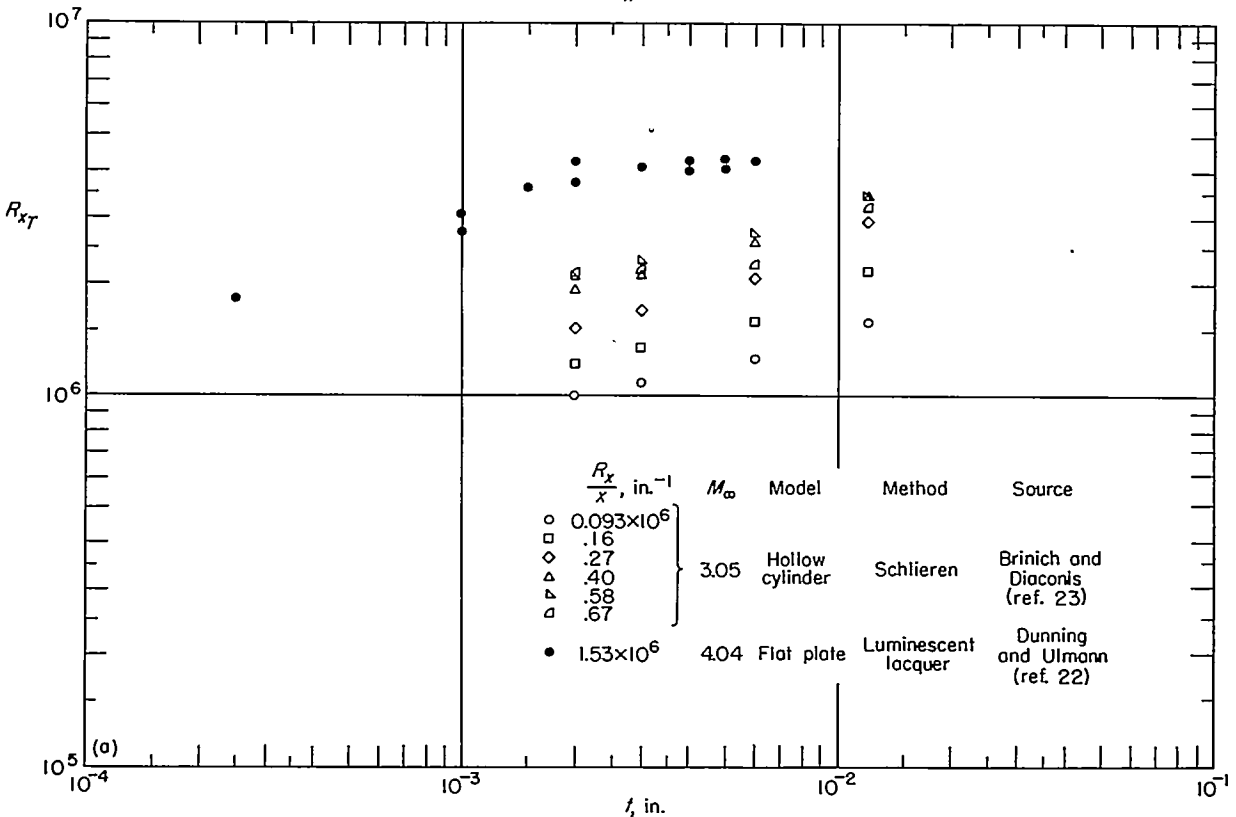
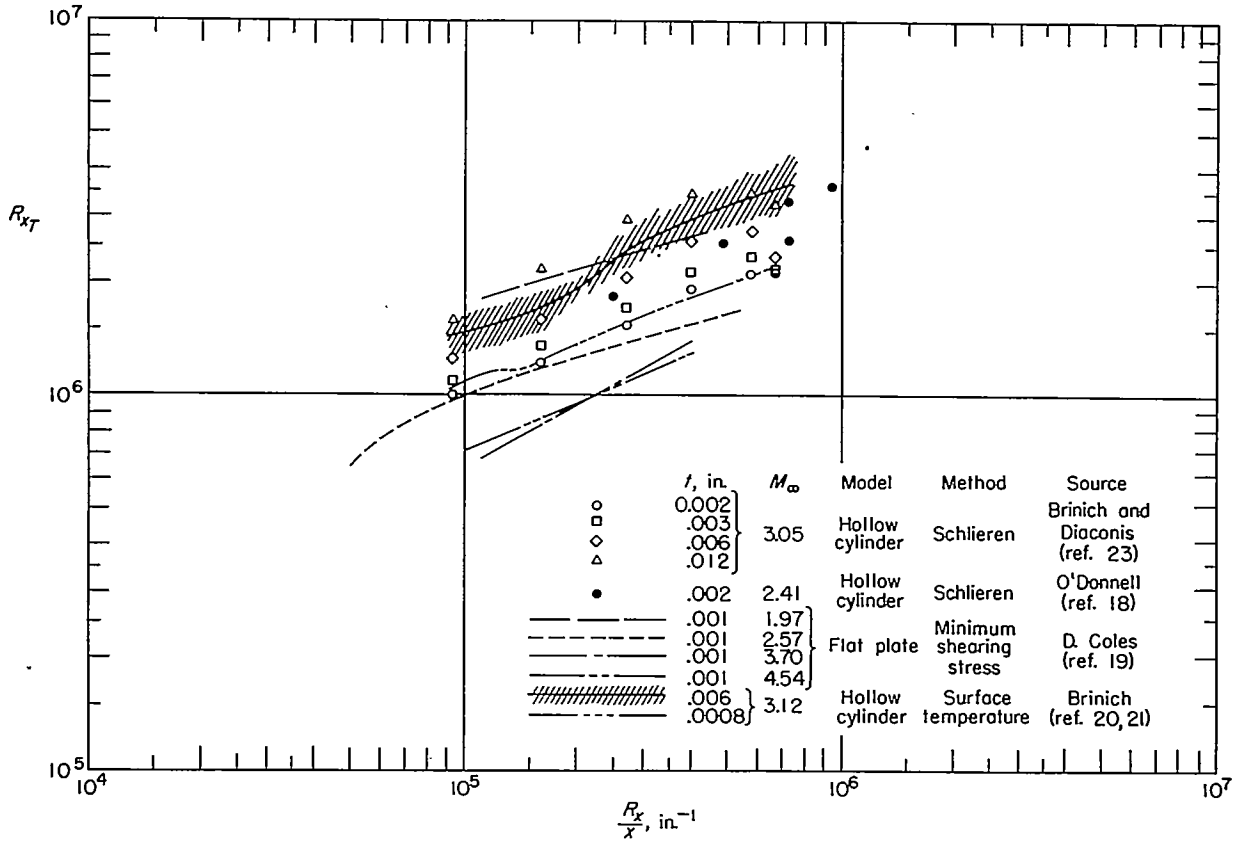
Certain of the datum points indicated in figure 10 are affected by the leading-edge shock as reflected from the tunnel wall and these points are given little weight. Other data points obtained from reference 25 ( $R_l$  of 260, 1,500, and 8,000) appear to be affected by a wave impinging on the surface. This result is apparently attributable to an imperfection of the nozzle.

On the basis of the correlation presented in figures 9 and 10 a variation in leading-edge thickness by a factor of 3 would be expected to give a change in the transition Reynolds number of about 50 percent which is more than adequate to explain the anomalies shown on table I.

Probe effects.—Little is known about the influence of the probes on transition; however, the main effects on the boundary layer of the relatively small probes used in this investigation appear to be in the details of the measured profiles rather than in the evaluation of whether the boundary layer is laminar or turbulent. A discussion of this latter effect is presented in appendix B to this report.

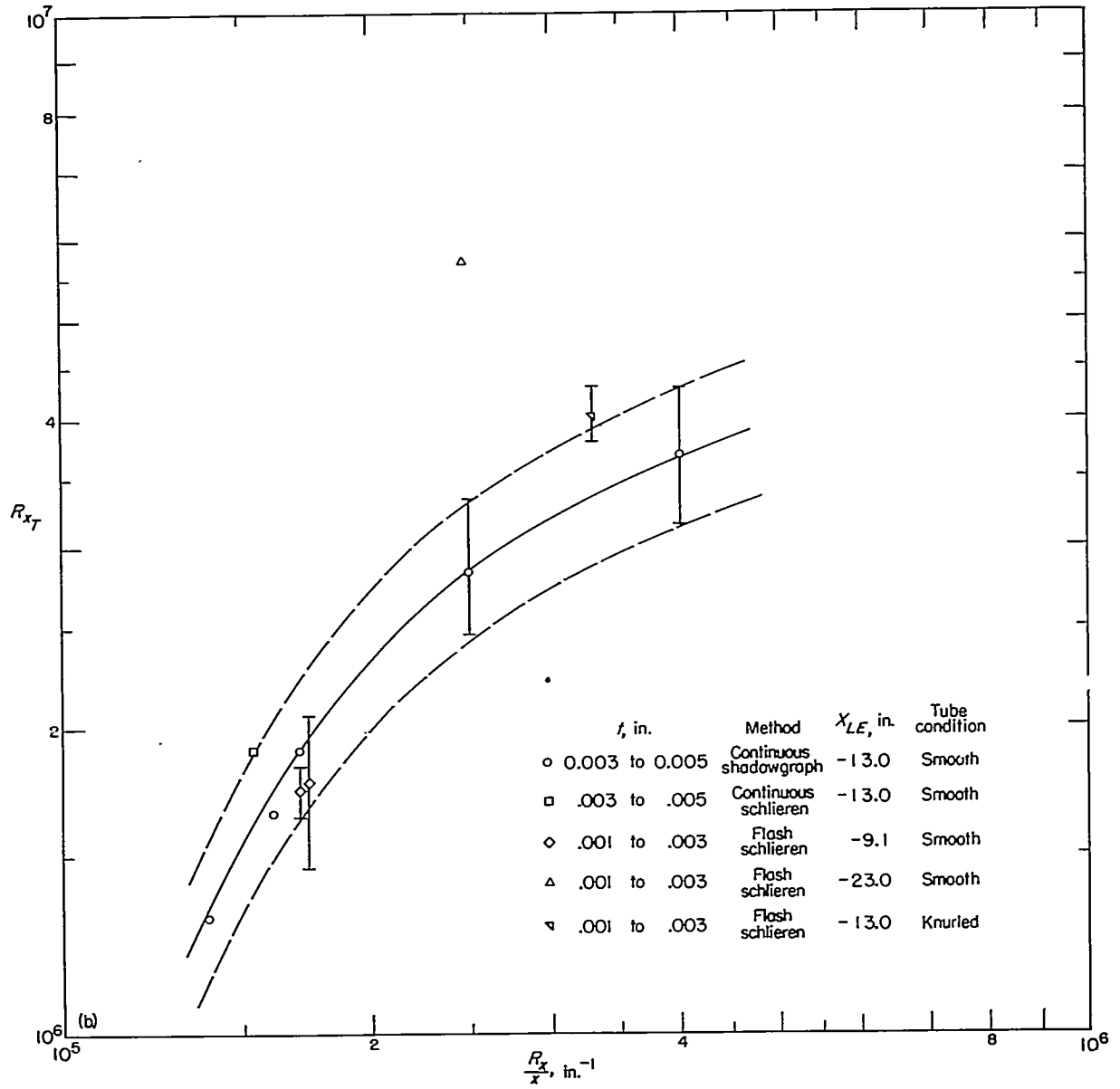
#### PRESSURE TESTS AT A LOWER PRESSURE LEVEL

A few pressure-survey tests were run on the smooth cylinder in the steel and Invar nozzles at a Reynolds number per inch of  $0.26 \times 10^6$  ( $p_t \approx 25$  atmospheres). These data are not as comprehensive as the data presented in figure 6 and thus do not justify presentation. Transition, according to these total-pressure profiles, was found to occur between a Reynolds number of  $4 \times 10^6$  and  $4.5 \times 10^6$  (corresponding to  $X_{LE}$  from  $-16$  to  $-18$  inches) in both the steel and the Invar nozzles. The wall temperatures for these tests are expected to be slightly below the values estimated for the higher pressure tests because of the reduced heat transfer.



(a) Previously available data.

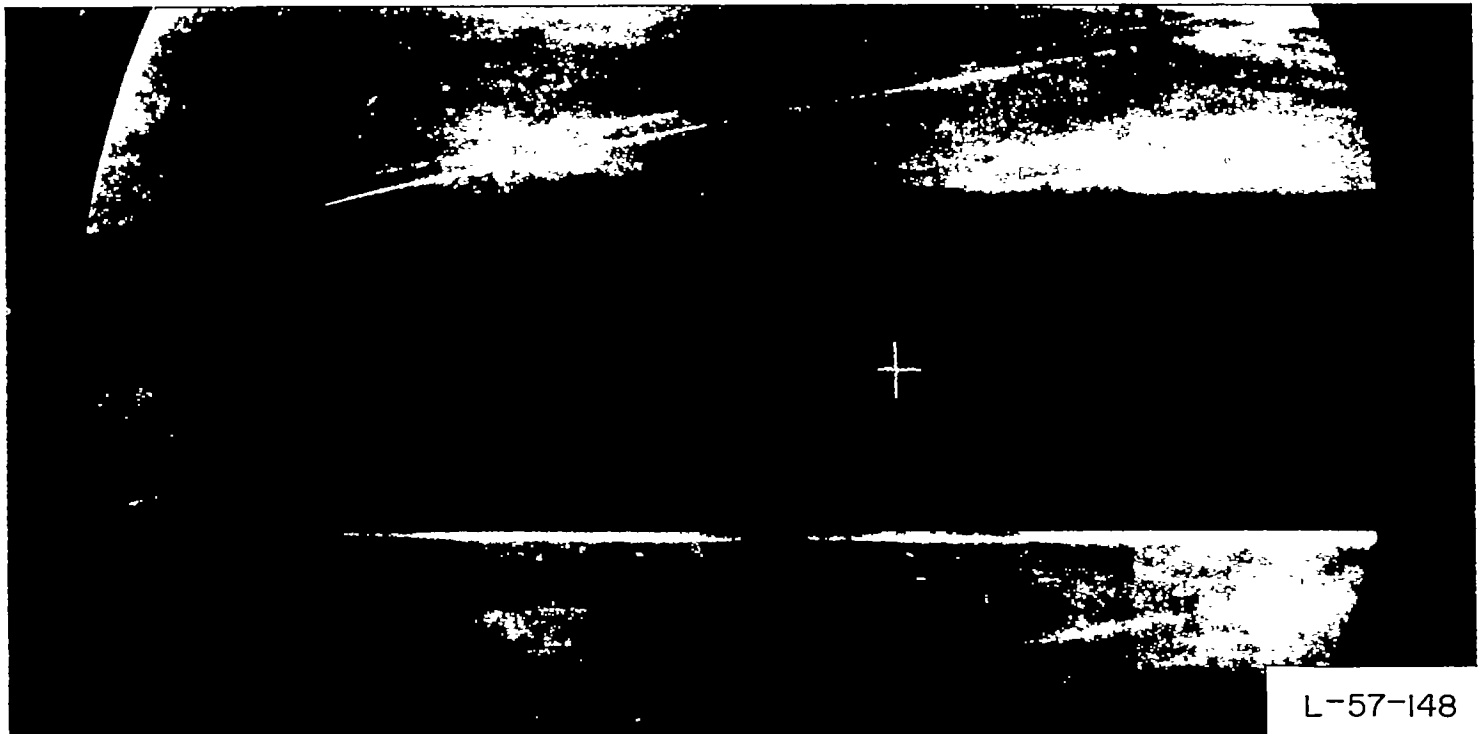
FIGURE 7.—The Reynolds numbers for transition on hollow cylinders and flat plates as a function of Reynolds number per inch and leading-edge thickness.



(b) Data from present tests with steel nozzle.  $M_\infty = 6.7$  to  $6.9$ .

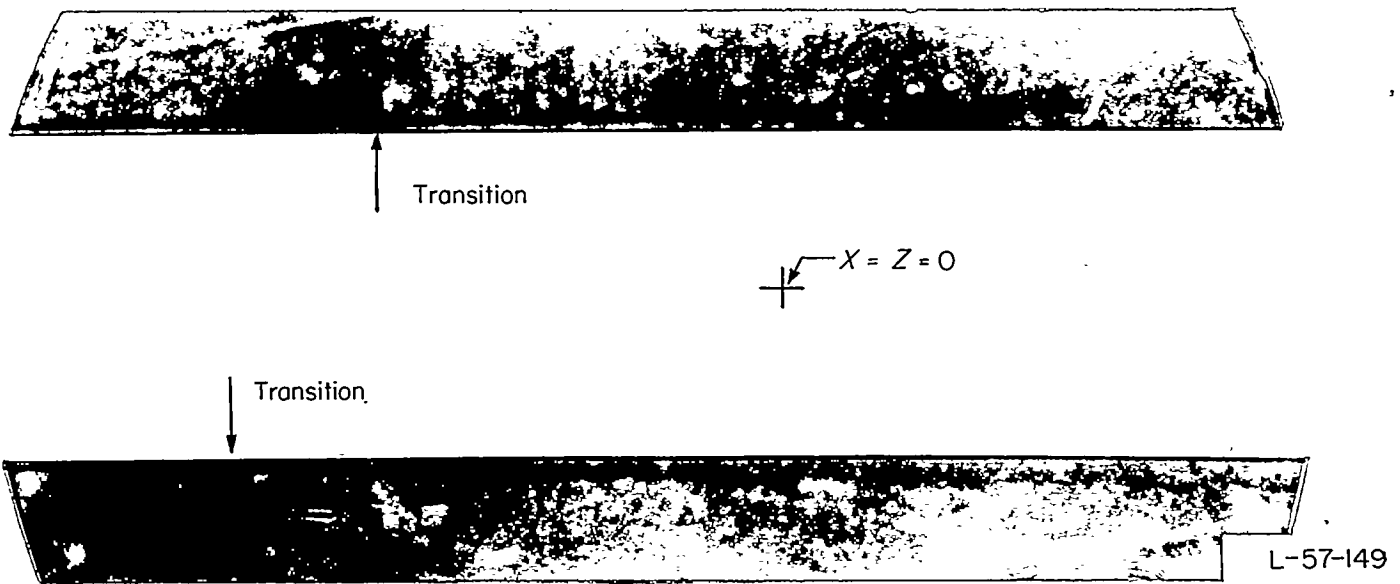
FIGURE 7.—Concluded.





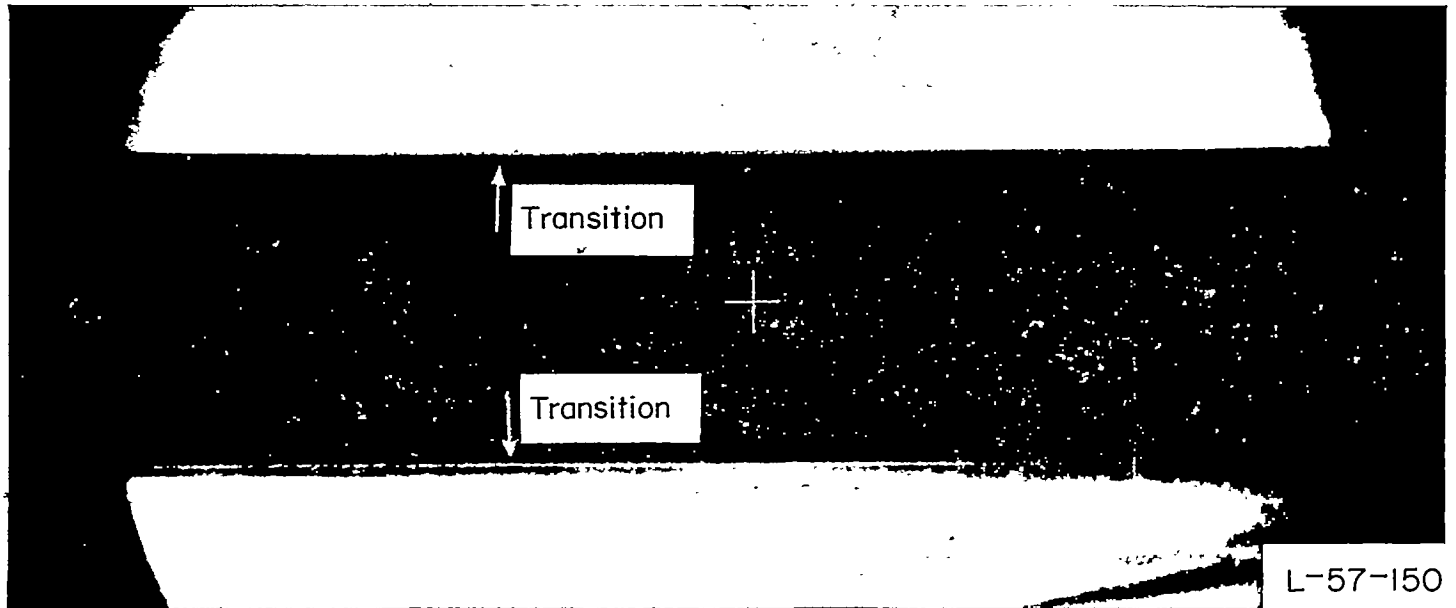
(a) Flash schlieren;  $R_x/x = 0.27 \times 10^6$  per inch;  $X_{LE} = -5.0$  inches;  $t = 0.001$  to  $0.003$  inch.

FIGURE 8.—Photographs by various methods of the flow over the hollow cylinder at various conditions.  $M_\infty \approx 6.9$ . All photographs in steel nozzle. Flow from left to right.

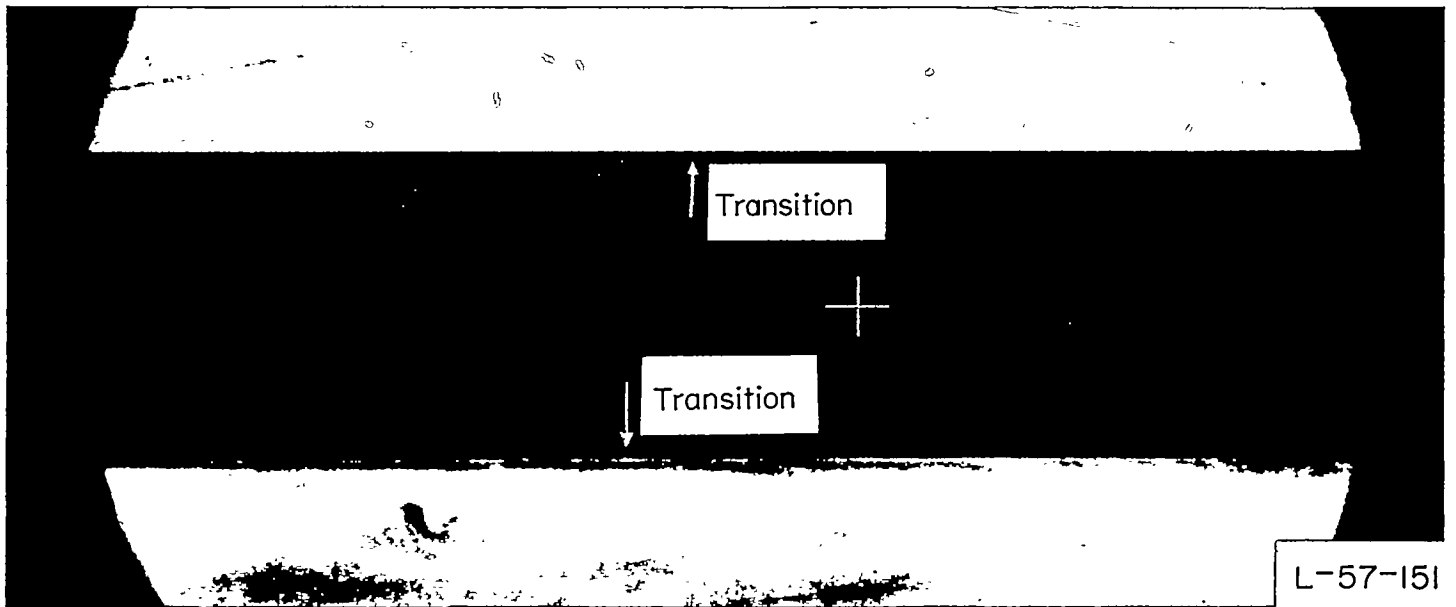


(b) Continuous shadowgraph;  $R_x/x = 0.47 \times 10^6$  per inch;  $X_{LE} = -13.0$  inches;  $t = 0.003$  to  $0.005$  inch.

FIGURE 8.—Continued.

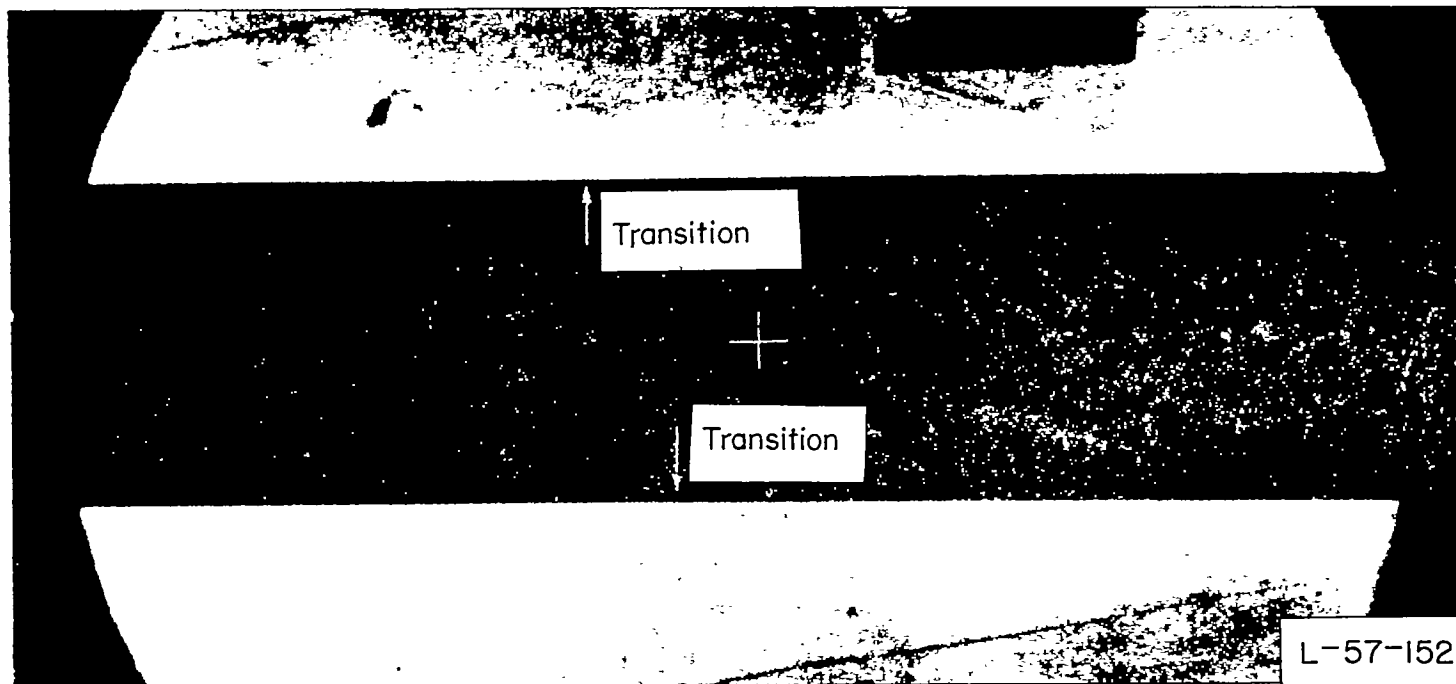


(c) Continuous schlieren;  $R_x/x = 0.26 \times 10^6$  per inch;  $X_{LE} = -13.0$  inches;  $t = 0.003$  to  $0.005$  inch.

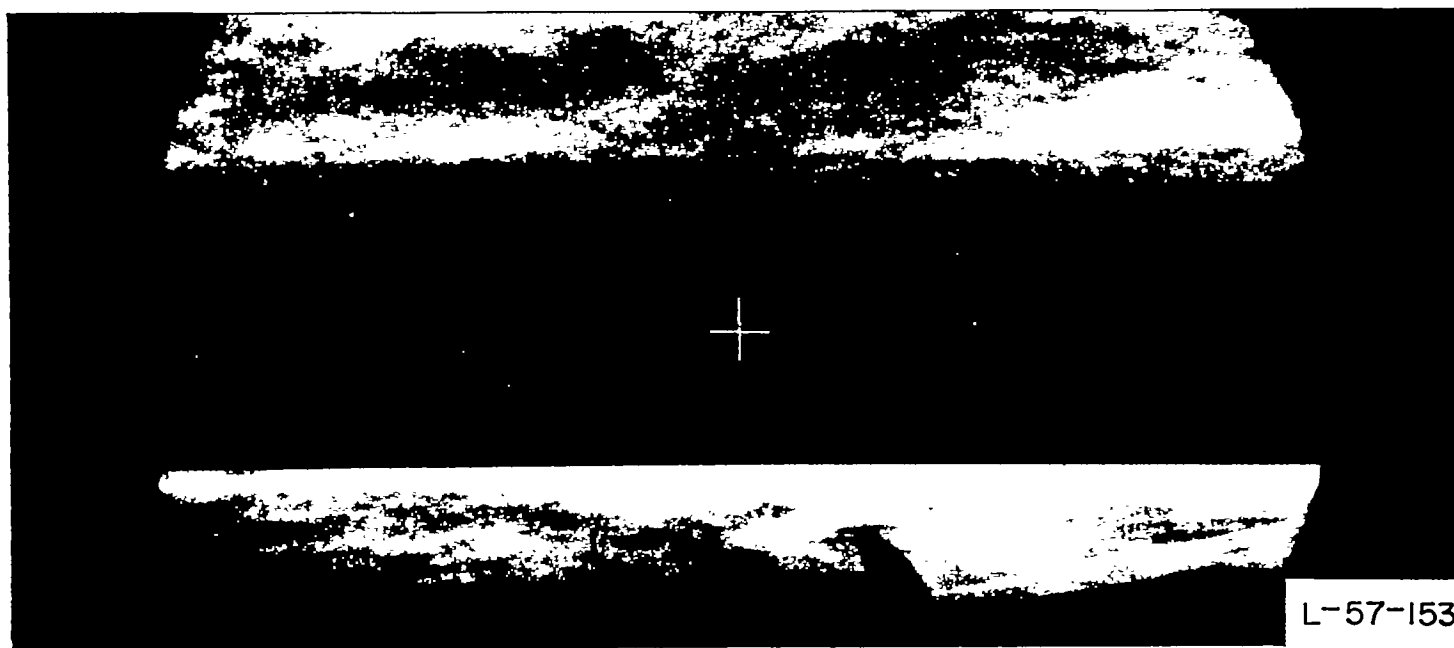


(d) Flash schlieren;  $R_x/x = 0.28 \times 10^6$  per inch;  $X_{LE} = -9.1$  inches;  $t = 0.001$  to  $0.003$  inch.

FIGURE 8.—Continued.



(e) Flash schlieren;  $R_x/x = 0.27 \times 10^6$  per inch;  $X_{LE} = -23.0$  inches;  $t = 0.001$  to  $0.003$  inch.



(f) Flash schlieren;  $R_x/x = 0.36 \times 10^6$  per inch;  $X_{LE} = -23.1$  inches;  $t = 0.001$  to  $0.003$  inch, knurled near leading edge.

FIGURE 8.—Continued.



(g) Flash schlieren;  $R_x/x = 0.23 \times 10^6$  per inch;  $X_{LE} = -18.0$  inches;  $t = 0.003$  to  $0.005$  inch.

FIGURE 8.—Concluded.

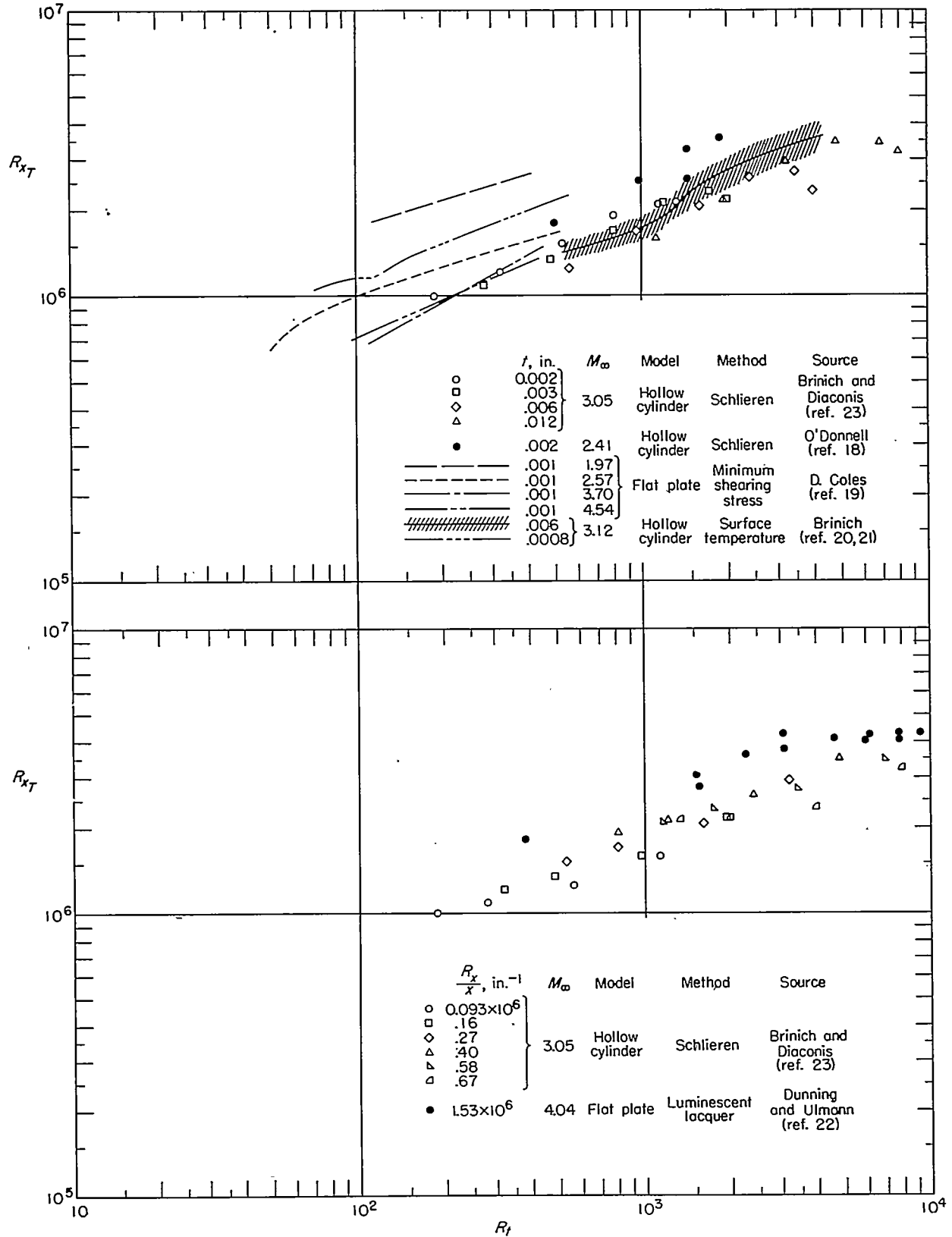


FIGURE 9.—The Reynolds numbers for transition on hollow cylinders and flat plates as a function of Reynolds number based on leading-edge thickness.

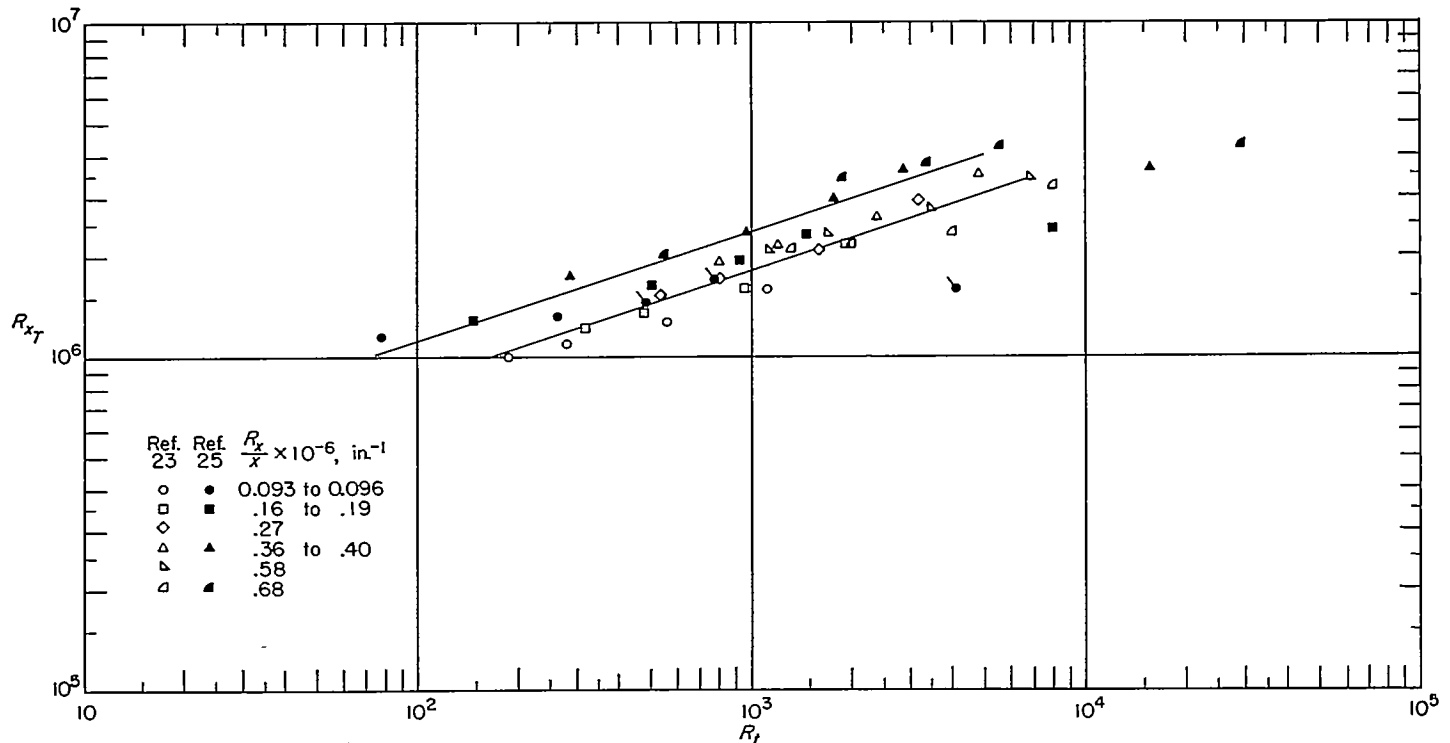


FIGURE 10.—The effect on the Reynolds number for transition of variations in the parameter Reynolds number based on leading-edge thickness at various pressure levels in the Lewis 1- by 1-foot variable Reynolds number wind tunnel. Flagged symbols affected by reflection of leading-edge shock.

**COMPARISON WITH OTHER RESULTS**

The tests by Korkegi (ref. 28) at  $M_\infty = 5.8$  on an insulated flat plate and Lee (ref. 29) at Mach numbers up to 5.0 on a hollow cylinder are perhaps the only wind-tunnel tests for boundary-layer transition on models with essentially zero pressure gradient at Mach numbers approaching those of the present investigation. However, it is difficult to compare the results of these investigations with the present results since their surface heating effects are different from those of the present tests and their model-leading-edge thicknesses are not given.<sup>2</sup> Nevertheless, since there is a dearth of high Mach number transition data, the results from these sources are presented.

In Korkegi's experiments (ref. 28) the Reynolds number per inch varied from about  $0.07 \times 10^6$  to  $0.23 \times 10^6$  with a corresponding variation in plate Reynolds number from about  $1.8 \times 10^6$  to greater than  $5 \times 10^6$ . Natural transition was not detected anywhere in this range. In the tests by Lee (ref. 29) the Mach number was varied from 2.15 to 5.01 with a corresponding variation in Reynolds number per inch

<sup>2</sup> Dr. Korkegi stated in a personal discussion with the author that he believed that the leading-edge thickness of the plate for the investigation reported in reference 28 was between 0.001 and 0.002 inch. If this was the case, then the Reynolds number based on leading-edge thickness for his tests varied over a range of values from about 100 to 400.

from roughly  $0.3 \times 10^6$  to  $0.07 \times 10^6$  (constant supply pressure). The Reynolds number per inch at  $M_\infty = 5.0$  is considerably lower than the lowest Reynolds number per inch of the present tests. Whether heat transfer was present is not stated, although the data were obtained in an intermittent tunnel with short test durations (approximately 35-second runs) and some heat transfer from the model to the boundary layer might occur. Lee's results show the transition Reynolds number in general to decrease with increasing Mach number to a value of about  $10^6$  at  $M_\infty = 5$ , with a scatter of about  $\pm 20$  percent. A different cylinder was used for the tests at the high Mach numbers so that it cannot be assumed that the leading-edge thickness was constant for all the tests.

**CONCLUDING REMARKS**

The Reynolds number for transition on the outside of a hollow cylinder has been investigated at a Mach number of 6.9 in the Langley 11-inch hypersonic tunnel. In these tests there was heat transfer from the boundary layer to the wall. The ratio of wall temperature to free-stream temperature  $T_w/T_\infty$  was believed to be an average of about 6.6 at the measuring stations, whereas  $T_w/T_\infty$  would be expected to be about 9.0 for the laminar boundary layer on an insulated

plate under the same conditions. The nature of the boundary layer was determined from impact-pressure surveys through the boundary layer and by optical viewing.

The data from pressure surveys obtained at a Reynolds number per inch of  $0.34 \times 10^6$ , with a leading-edge thickness varying between 0.001 inch and 0.003 inch around the circumference of the leading edge, in a portion of the nozzle where surveys had shown the Mach number variation to be small, indicated a transition Reynolds number of about  $4 \times 10^6$ , although some profiles indicated higher and others, lower values. When the cylinder protruded into a region of the nozzle with a considerable negative pressure gradient, the Reynolds number for transition was increased and for one set of data appeared to approach  $8 \times 10^6$ .

Data obtained optically on a similar cylinder with a leading-edge thickness in the range from 0.003 to 0.005 inch indicated a Reynolds number for transition varying from about  $1.3 \times 10^6$  at a Reynolds number per inch of  $0.14 \times 10^6$  to about  $3.7 \times 10^6$  at a Reynolds number per inch of  $0.4 \times 10^6$ . As with the data obtained from pressure surveys an anomalous result was obtained for one run in which the leading

edge of the cylinder with a slightly thinner leading edge protruded far upstream in the nozzle. In this case a Reynolds number for transition of about  $5.7 \times 10^6$  was obtained at a Reynolds number per inch of about  $0.25 \times 10^6$ .

From a correlation of results obtained at lower Mach numbers (Mach numbers in the range 2.0 to 4.5) and data from the present tests with variable Reynolds number per inch, the leading-edge thickness and free-stream Reynolds number per inch appear to be important considerations in flat-plate transition results. Results from various installations would not appear to be comparable unless these factors are taken into account. At a given Mach number it appears that the Reynolds number based on leading-edge thickness is a significant parameter that must be considered in comparisons of flat-plate or hollow-cylinder transition data from various facilities.

LANGLEY AERONAUTICAL LABORATORY,  
NATIONAL ADVISORY COMMITTEE FOR AERONAUTICS,  
LANGLEY FIELD, VA., *February 9, 1956.*

**APPENDIX A**

**THEORETICAL BOUNDARY-LAYER PROFILES**

In order to determine the effect of the various variable or imperfectly known conditions on the profiles to be examined, theoretical calculations of the effects of some of these conditions were made.

**EFFECT OF WALL TEMPERATURE ON LAMINAR PROFILES**

In order to assess the effect of various wall temperatures on the shape of the total-pressure, Mach number, and velocity profiles on the laminar boundary layer, calculations were made by the Crocco method as presented by Van Driest (ref. 15) for free-stream conditions close to those of the present tests. The surface was assumed isothermal with a constant-pressure flow field, and the Prandtl number and specific heats were taken as invariant through the boundary layer. The computations were carried out to a velocity ratio in the boundary layer of 0.999. The results of these calculations are shown in figure 11. Qualitatively, for the range of surface temperatures shown, the effect on the general profile shapes of changes in surface temperature is small.

**EFFECT OF PRANDTL NUMBER ON LAMINAR PROFILES**

In order to assess the effect of various Prandtl numbers on the shape of the total-pressure, Mach number, and velocity profiles on the laminar boundary layer, calculations were again made according to reference 15. The results are presented in figure 12. The assumptions are the same as in the preceding paragraph except that the plate is assumed to have an insulated surface. Again for the present purposes the effect of Prandtl number is found to be minor.

**EFFECT OF EXPONENT IN POWER LAW FOR VELOCITY ON PROFILE SHAPE**

If the linear velocity profile is assumed to approximate the velocities in a laminar boundary layer (see figs. 11 and 12) and the turbulent boundary layer is represented by a velocity varying as the 1/6 to 1/7 power of distance from the surface of an insulated plate (refs. 28 and 30), the pitot pressure, Mach number, and velocity profiles shown in figure 13 are obtained for a Prandtl number of 1.0.

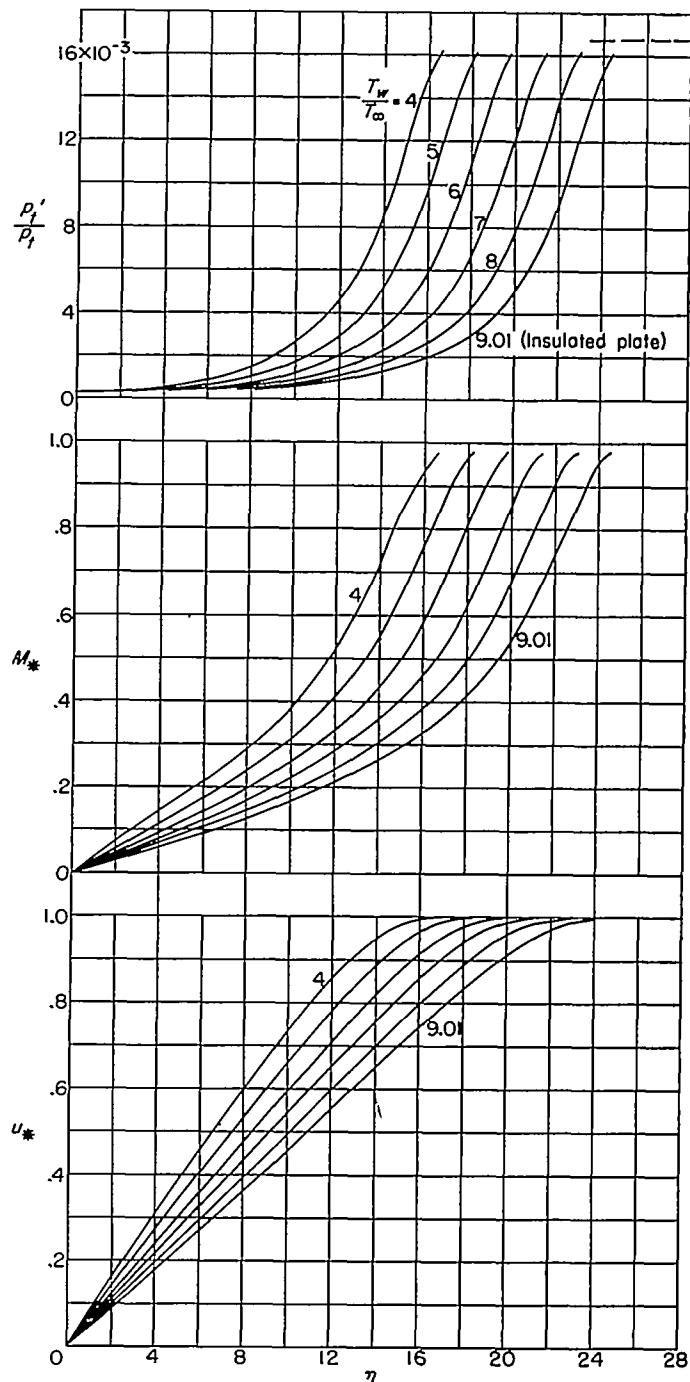


FIGURE 11.—Effect of wall temperature on profiles of flat-plate laminar boundary layer.  $M_\infty = 6.86$ ;  $T_\infty = 111^\circ \text{R}$ ;  $N_{Pr} = 0.725$ .



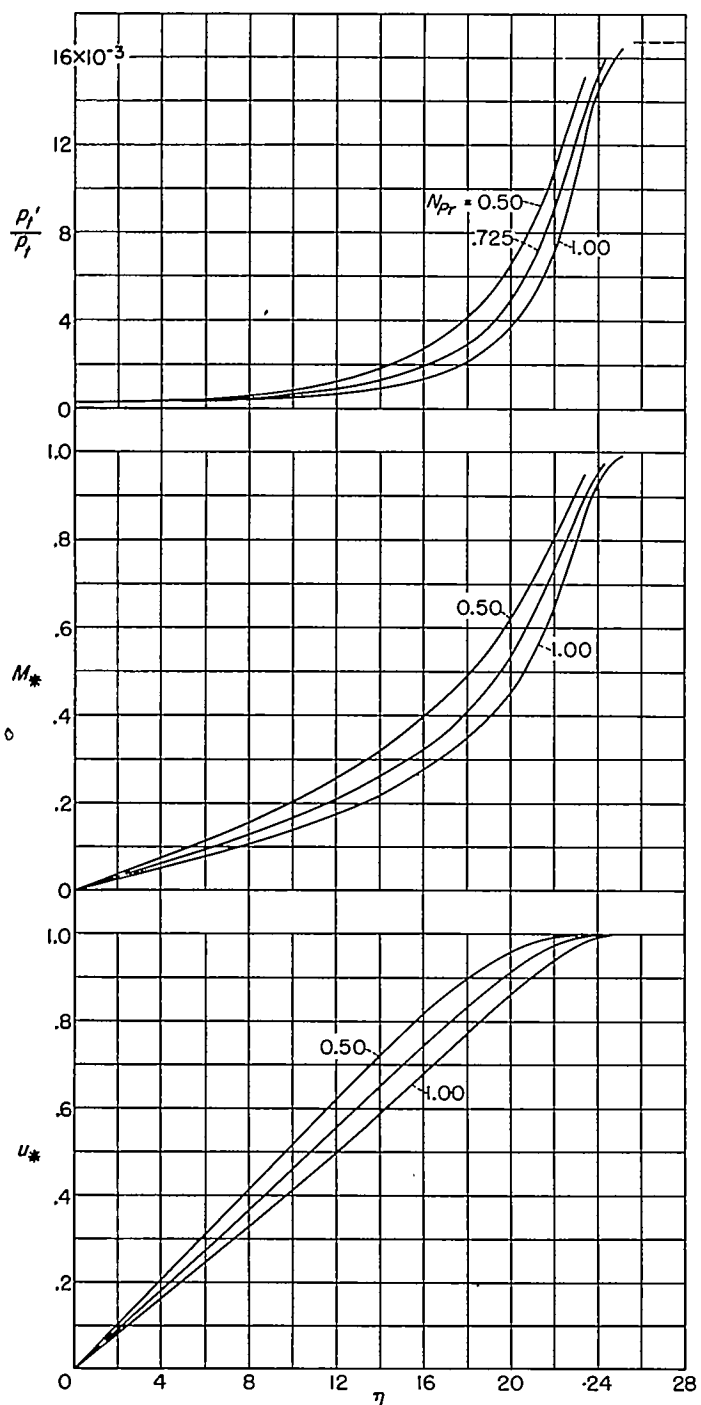


FIGURE 12.—Effect of Prandtl number on profiles in laminar boundary layer on insulated flat plate.  $M_\infty = 6.86$ ;  $T_\infty = 111^\circ \text{ R}$ .

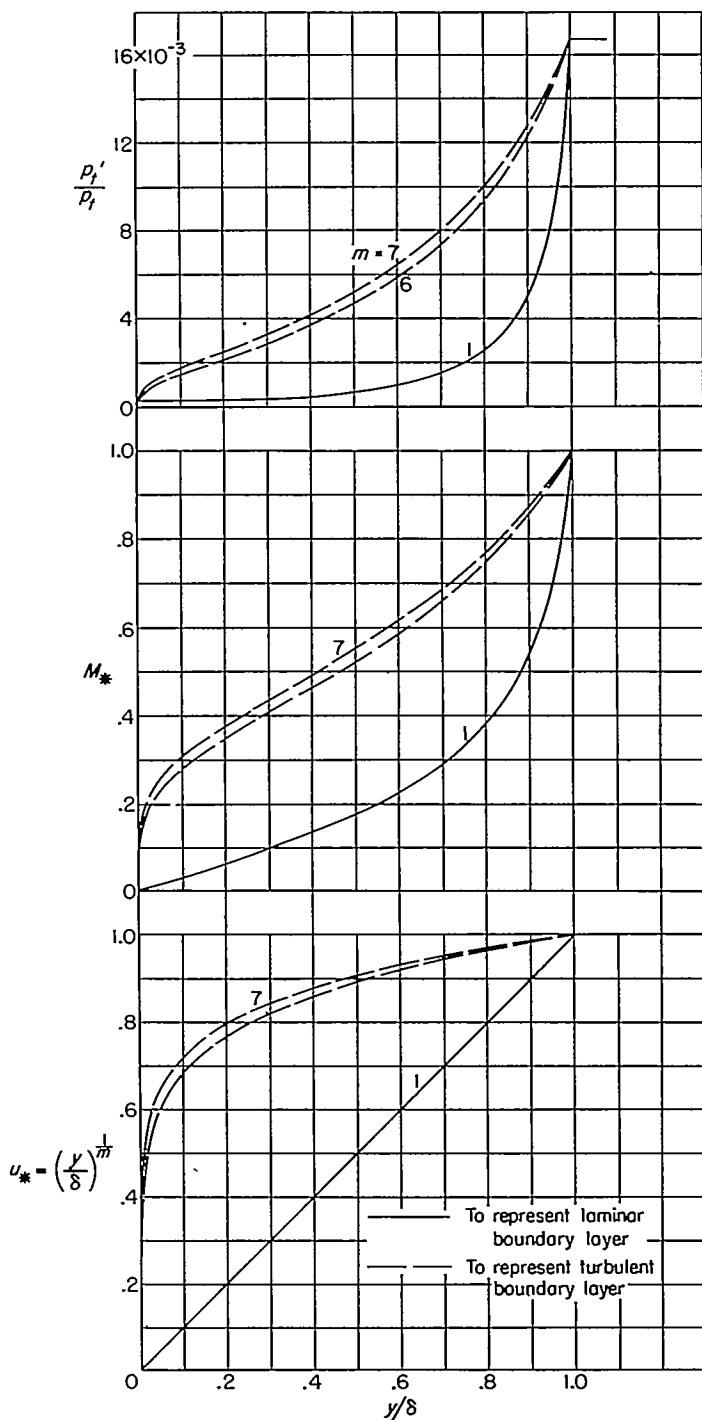


FIGURE 13.—Effect of assumed velocity profile on Mach number and total-pressure profiles in boundary layer.  $M_\infty = 6.86$ ;  $N_{Pr} = 1.00$ .

## APPENDIX B

### PROBE EFFECTS

The impact pressure and velocity profiles presented in figure 6 indicate two regions of disagreement between the laminar theory and the experimental results that were classed as laminar: the first is near the model surface (best shown by the velocities); the second is near the outer edge of the boundary layer (shown by the impact-pressure results).

A probe situated very near a wall can introduce errors of various sorts in the measured pressures. Among these are the following:

(a) Distortion due to the existence of high velocity gradients near the wall.

(b) Viscous effects at the probe nose resulting because the Reynolds numbers in the subsonic part of the laminar boundary layer can be several orders of magnitude reduced from free-stream values (illustrated by fig. 14).

(c) Initiation of separation resulting from the presence of the probe (as observed by Morkovin and Bradfield, ref. 31).

The measurements of Taylor (ref. 32) using Stanton type surface tubes and von Doenhoff (ref. 33) using flattened-tip total-pressure tubes in contact with the surface bear on the overall effect of all these factors on the measured pitot pressure. Their results indicate that the indicated impact pressure in the present tests can be 10 to 15 percent higher than boundary-layer theory would give. This increase in impact pressure results in an indicated increase in  $u^*$  of perhaps 0.15 or 0.2, which is the magnitude of the effects shown in figure 6(a) by the data taken near the wall.

In addition to the effects previously discussed, attention is directed to figure 6(b) (steel nozzle, circle and square symbols) and figure 6(d) (steel nozzle, circle symbol), where the distortion of the profile extends into the supersonic portion of the boundary layer. This effect is apparently caused by the onset of transition and resembles an effect shown in certain of the profiles presented by Korkegi (ref. 28, fig. 24) and is not attributable in its main features to the influence of the probe. Transition as shown by this profile in figure 6(d) is considered to be slightly more advanced than that of figure 6(b); however, from a comparison with the theoretical laminar profiles, in both cases transition is considered to be in the incipient stage.

The deviation of experimental impact-pressure ratio from the theoretical value near the outer edge of the boundary

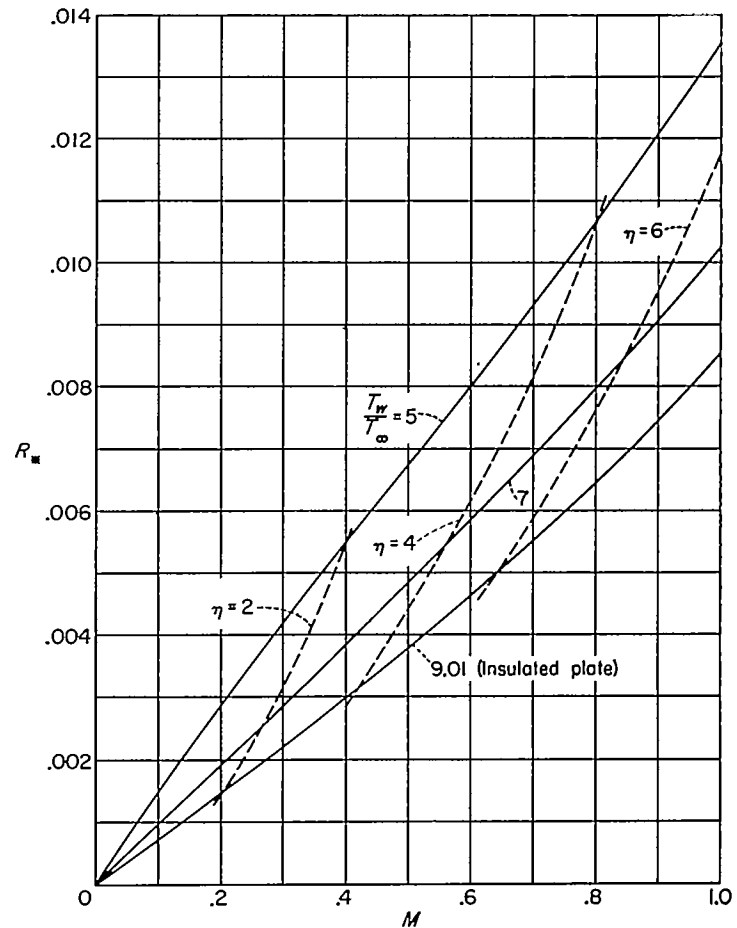


FIGURE 14.—The variation of local Reynolds number parameter with local Mach number at various wall temperatures in the subsonic part of a laminar boundary layer.  $M_\infty=6.86$ ;  $T_\infty=111^\circ\text{R}$ ;  $N_{Pr}=0.725$

layer (fig. 6(a) steel nozzle, especially) may be due partly to the finite thickness of the leading edge. Qualitatively, such deviations as this were found by Bradfield, Decoursin, and Blumer at  $M_\infty=3.05$  (ref. 24, fig. 6) to be due to increasing the leading-edge thickness. Another possible explanation is an inadequacy in flat-plate theory as applied to a cylinder and, in addition, there are certain terms in the solution to the boundary-layer equations which can be significant near the outer edge of the boundary layer and which were neglected in the computations of the theory.

REFERENCES

1. Lees, Lester, and Lin, Chia Chiao: Investigation of the Stability of the Laminar Boundary Layer in a Compressible Fluid. NACA TN 1115, 1946.
2. Lees, Lester: The Stability of the Laminar Boundary Layer in a Compressible Fluid. NACA Rep. 876, 1947. (Supersedes NACA TN 1360.)
3. Van Driest, E. R.: Calculation of the Stability of the Laminar Boundary Layer in a Compressible Fluid on a Flat Plate With Heat Transfer. Jour. Aero. Sci., vol. 19, no. 12, Dec. 1952, pp. 801-812.
4. Dunn, D. W., and Lin, C. C.: On the Stability of the Laminar Boundary Layer in a Compressible Fluid. Jour. Aero. Sci., vol. 22, no. 7, July 1955, pp. 455-477.
5. Potter, J. L.: Friction Drag and Transition Reynolds Number on Bodies of Revolution at Supersonic Speeds. NAVORD Rep. 2150, U. S. Naval Ord. Lab. (White Oak, Md.), Aug. 20, 1951.
6. McLellan, Charles H.: Exploratory Wind-Tunnel Investigation of Wings and Bodies at  $M=6.9$ . Jour. Aero. Sci., vol. 18, no. 10, Oct. 1951, pp. 641-648.
7. Bertram, Mitchel H.: An Approximate Method for Determining the Displacement Effects and Viscous Drag of Laminar Boundary Layers in Two-Dimensional Hypersonic Flow. NACA TN 2773, 1952.
8. Potter, J. L.: New Experimental Investigations of Friction Drag and Boundary Layer Transition on Bodies of Revolution at Supersonic Speeds. NAVORD Rep. 2371, U. S. Naval Ord. Lab. (White Oak, Md.), Apr. 24, 1952.
9. Gazley, Carl, Jr.: Boundary-Layer Stability and Transition in Subsonic and Supersonic Flow. A Review of Available Information With New Data in the Supersonic Range. Jour. Aero. Sci., vol. 20, no. 1, Jan. 1953, pp. 19-28.
10. Czarnecki, K. R., and Sinclair, Archibald R.: Factors Affecting Transition at Supersonic Speeds. NACA RM L53I18a, 1953.
11. Czarnecki, K. R., and Sinclair, Archibald R.: An Investigation of the Effects of Heat Transfer on Boundary-Layer Transition on a Parabolic Body of Revolution (NACA RM-10) at a Mach Number of 1.61. NACA Rep. 1240, 1954. (Supersedes NACA TN's 3165 and 3166.)
12. McLellan, Charles H., Williams, Thomas W., and Bertram, Mitchel H.: Investigation of a Two-Step Nozzle in the Langley 11-Inch Hypersonic Tunnel. NACA TN 2171, 1950.
13. McLellan, Charles H., Williams, Thomas W., and Beckwith, Ivan E.: Investigation of the Flow Through a Single-Stage Two-Dimensional Nozzle in the Langley 11-Inch Hypersonic Tunnel. NACA TN 2223, 1950.
14. Jedlicka, James R., Wilkins, Max E., and Seiff, Alvin: Experimental Determination of Boundary-Layer Transition on a Body of Revolution at  $M=3.5$ . NACA TN 3342, 1954.
15. Van Driest, E. R.: Investigation of Laminar Boundary Layer in Compressible Fluids Using the Crocco Method. NACA TN 2597, 1952.
16. Lee, R. E.: Measurements of Blockage Area Ratio, Pressure Distribution, and Boundary Layer Transition on Hollow Cylinders. NAVORD Rep. 3650 (Aeroballistic Res. Rep. 226), U. S. Naval Ord. Lab., Mar. 8, 1954.
17. Bertram, Mitchel H.: Viscous and Leading-Edge Thickness Effects on the Pressures on the Surface of a Flat Plate in Hypersonic Flow. Jour. Aero. Sci. (Readers' Forum), vol. 21, no. 6, June 1954, pp. 430-431.
18. O'Donnell, Robert M.: Experimental Investigation at a Mach Number of 2.41 of Average Skin-Friction Coefficients and Velocity Profiles for Laminar and Turbulent Boundary Layers and an Assessment of Probe Effects. NACA TN 3122, 1954.
19. Coles, Donald: Measurements of Turbulent Friction on a Smooth Flat Plate in Supersonic Flow. Jour. Aero. Sci., vol. 21, no. 7, July 1954, pp. 433-448.
20. Brinich, Paul F.: Boundary-Layer Transition at Mach 3.12 With and Without Single Roughness Elements. NACA TN 3267, 1954.
21. Brinich, Paul F.: A Study of Boundary-Layer Transition and Surface Temperature Distributions at Mach 3.12. NACA TN 3509, 1955.
22. Dunning, Robert W., and Ulmann, Edward F.: Effects of Sweep and Angle of Attack on Boundary-Layer Transition on Wings at Mach Number 4.04. NACA TN 3473, 1955.
23. Brinich, Paul F., and Diaconis, Nick S.: Boundary-Layer Development and Skin Friction at Mach Number 3.05. NACA TN 2742, 1952.
24. Bradfield, W. S., Decoursin, D. G., and Blumer, C. B.: The Effect of Leading-Edge Bluntness on a Laminar Supersonic Boundary Layer. Jour. Aero. Sci., vol. 21, no. 6, June 1954, pp. 373-382, 398.
25. Brinich, Paul F.: Effect of Leading-Edge Geometry on Boundary-Layer Transition at Mach 3.1. NACA TN 3659, 1956.
26. Ross, Albert O.: Determination of Boundary-Layer Transition Reynolds Numbers by Surface-Temperature Measurement of a  $10^\circ$  Cone in Various NACA Supersonic Wind Tunnels. NACA TN 3020, 1953.
27. Evvard, John C., Tucker, Maurice, and Burgess, Warren C., Jr.: Statistical Study of Transition-Point Fluctuations in Supersonic Flow. NACA TN 3100, 1954.
28. Korkegi, R. H.: Transition Studies and Skin-Friction Measurements on an Insulated Flat Plate at a Mach Number of 5.8. Jour. Aero. Sci., vol. 23, no. 2, Feb. 1956, pp. 97-107, 192.
29. Lee, Roland E.: Measurements of Pressure Distribution and Boundary-Layer Transition on a Hollow-Cylinder Model. NAVORD Rep. 2823 (Aeroballistic Res. Rep. 176), U. S. Naval Ord. Lab. (White Oak, Md.), Apr. 23, 1953.
30. Lobb, R. Kenneth, Winkler, Eva M., and Persh, Jerome: Experimental Investigation of Turbulent Boundary Layers in Hypersonic Flow. Jour. Aero. Sci., vol. 22, no. 1, Jan. 1955, pp. 1-9, 50.
31. Morkovin, M. V., and Bradfield, W. S.: Probe Interference in Measurements in Supersonic Laminar Boundary Layers. Jour. Aero. Sci. (Readers' Forum), vol. 21, no. 11, Nov. 1954, pp. 785-787.
32. Taylor, G. I.: Measurements With a Half-Pitot Tube. Proc. Roy. Soc. (London), ser. A, vol. 166, no. 927, June 16, 1938, pp. 476-481.
33. Von Doenhoff, Albert E.: Investigation of the Boundary Layer About a Symmetrical Airfoil in a Wind Tunnel of Low Turbulence. NACA WR L-507, 1940. (Formerly NACA ACR, Aug. 1940.)

